CATALYTIC BEHAVIORS OF FE-MN MIXED OXIDES

NATIONAL TAIWAN UNIV., TAIPEI

1988

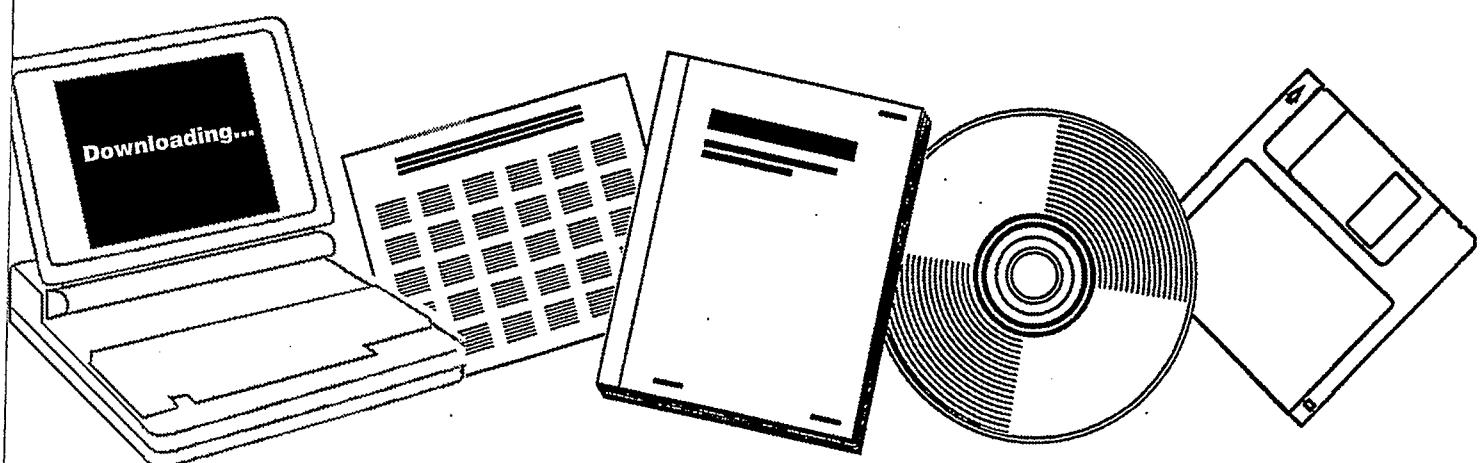

One Source. One Search. One Solution.

NTIS

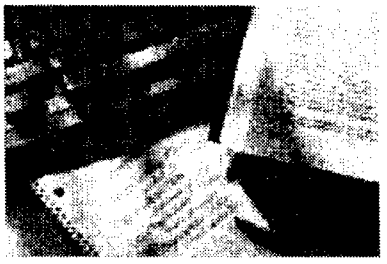

Providing Permanent, Easy Access to U.S. Government Information

National Technical Information Service is the nation's largest repository and disseminator of government-initiated scientific, technical, engineering, and related business information. The NTIS collection includes almost 3,000,000 information products in a variety of formats: electronic download, online access, CD-ROM, magnetic tape, diskette, multimedia, microfiche and paper.

Search the NTIS Database from 1990 forward

NTIS has upgraded its bibliographic database system and has made all entries since 1990 searchable on **www.ntis.gov.** You now have access to information on more than 600,000 government research information products from this web site.

Link to Full Text Documents at Government Web Sites

Because many Government agencies have their most recent reports available on their own web site, we have added links directly to these reports. When available, you will see a link on the right side of the bibliographic screen.

Download Publications (1997 - Present)

NTIS can now provides the full text of reports as downloadable PDF files. This means that when an agency stops maintaining a report on the web, NTIS will offer a downloadable version. There is a nominal fee for each download for most publications.

For more information visit our website:

www.ntis.gov

U.S. DEPARTMENT OF COMMERCE
Technology Administration
National Technical Information Service
Springfield, VA 22161

Catalytic Behaviors of Fe-Mn Mixed Oxides

Author: Lee, Min-Ta

National Science Council
Taiwan, Republic of China

ABSTRACT

The effect of the addition of manganese oxide to iron catalyst for Fischer-Tröpsch reaction was studied by Mössbauer spectroscopy, X-ray diffraction, temperature programmed reduction and kinetic measurements. Catalysts before reduction are composed of binary oxide solid solutions such as $Fe_{2-x}Mn_xO_3$ and $Mn_{2-x}Fe_xO_3$ phases. Reduction of the catalysts proceeds via the formation of $Fe_{3-y}Mn_yO_4$, $Mn_{3-y}Fe_yO_4$ mixed spinel and $Fe_{1-z}Mn_zO$ mixed oxide to a-iron and MnO. Addition of manganese strongly stabilizes the intermediate oxidation state of catalysts thus prevents complete reduction. After the use for CO hydrogenation, catalysts are oxidized as well as carburized and complex phases results. Both oxidation and carburization are important in determining the catalytic behavior. Oxidation seems to be caused by water gas shift reaction. Different pretreatment procedure can produce different phases therefore results in different selectivity pattern. It is believed that $Mn_{3-y}Fe_yO_4$ mixed spinel and $Fe_{1-z}Mn_zO$ mixed oxide are the most powerful phases for olefin production. The highest attainable 2-4 low carbon olefin selectivity obtained is 41% on a 86% conversion level. Higher manganese content or lower reduction temperature may change the carbide formed to more unstable E'-$Fe_{2.2}C$ from X-Fe_5C_2. Carbide formation is greatly connected with manganese content and activation procedure used. It is speculated that more unstable carbide is necessary to produce more olefin.

Key words: Iron catalyst, Manganese, CO hydrogenation, Fischer-Tropsch synthesis.

CONTENTS

INTRODUCTION

The research of iron - manganese bimetallic catalysts on Fischer-Tropsch synthesis was initiated by the study of heat of adsorption of hydrogen and carbon monoxide on transition metals (1). From these experimental evidence, it was speculated that if it could add some manganese , the more effective CO activator , in iron, more effective olefin producing catalysts might be made. Accordingly, Bussemeier et al. (2) developed a high olefin producing Fe/Mn catalyst. Kobel (3) reported in 1979 a Fe/Mn=1/9 catalyst on which 2-4 low carbon olefin selectivity can be as high as 90% at a 70% conversion level. Bearns (4,5) studied the coprecipitated iron-manganese catalysts and found that there exists mixed lattice binary oxides such as $Fe_{2-x}Mn_xO_3$ or $Mn_{2-y}Fe_yO_3$ phases in the catalysts after subjected to high temperature calcination. In the subsequent reduction step, the Mn-rich phase is reduced via the formation of Mn_2FeO_4 spinel and wustite FeO to the metallic iron and manganese(II) oxide. The wustite phase is also enriched in manganese and another solid solution $Fe_{1-z}Mn_zO$ is formed. The results of the activity test showed that activity vs. time pattern depends greatly on the reduction temperature and the manganese content. Small amount of manganese has the effect of increasing the 2-4 low carbon olefin selectivity. Butt (6) showed from the study of Mossbauer spectroscopy the high Fe content catalysts (60%-80%) possesses two phases of binary oxide solid

solutions while low Fe content catalyst after high temperature calcination has only one single phase of $Mn_{2-y}Fe_yO_3$ binary oxide. During the reduction step, iron and manganese are always in a solid solution state, but there is no alloy in the final fully reduced or carburized catalysts. Phase composition of the used catalysts are highly dependent on reduction temperature. The low temperature reduced catalysts are mainly composed of $MnFe_2O_4$ while the high temperature reduced ones possess large amount of Hagg X-Fe_5C_2 carbides.

Mossoth (7,8) found the chemisorption of carbon monoxide and hydrogen on iron-manganese catalysts decreases drastically with increasing manganese content. Bearns (9) has also done a comprehensive study of chemisorption on manganese containing catalysts and found that the temperature at which chemisorption of carbon monoxide, hydrogen, and ethylene occurs is very different if the catalyst is reduced at different temperatures.

Barrault and Renard (10,11) prepared the iron-manganese catalysts by occlusion and impregnation of various iron salts on manganese oxide, and found that the catalyst Fe/Mn=1 has the highest olefin production ability. They also observed the drastic low amount of hydrogen chemisorption.

Iron-manganese bimetal catalyst can form very complex phases and its phase composition highly depends upon the calcination and the reduction temperature. Different activation procedure may result in totally different selectivity pattern. Several researchers employed the different pretreatment procedures to activate the catalyst, substantially different crystalline phase

compositions were obtained and totally different catalytic behaviors may result. Van. Dijk (12) reported that he did not observe the promoter effect of manganese. Up to now, there is still no conclusive explanation about the effect of addition of manganese. But it is speculated that the effect of manganese is not a simple surface electronic effect like potassium, the crystalline structure of the catalyst has to play some important role in it.

In this article, we have done a systematic study on a series of different compositions of iron-manganese coprecipitated catalysts. Mössbauer spectroscopy and X-ray diffraction were used to investigate the bulk crystalline structure. Catalyst tests were done using a integral high pressure fixed bed reactor, and along with TPR data, a model was proposed to correlate the catalytic properties and the catalyst structures.

EXPERIMENTAL:

(a) Catalyst preparation :

Five catalysts with molar ratios of iron to manganese, 1/0, 9/1, 1/1, 1/9, 0/1 respectively were prepared by coprecipitation method. The proper amounts of $Fe(NO3)._9H_2O$ and $Mn(NO_3).4H_2O$ (Merk GR grade) were taken into a kettle (Fig. 1) and deionized water was added to make a total 0.4 M solution. The 11% ammonia solution was prepared by diluting concentrated aqueous ammonia (Merk 33% extra pure) with deionized water, the amount of ammonia was about 25% in excess to precipitate the metal salts. The

kettle was heated in a constant temperature water bath to 90°C, and the ammonia solution was injected into the kettle by a mili pump (2 ml/min). After all the ammonia solution was injected to the kettle, the suspension was allowed to age for 2 hours, then it was hot filtered, washed with 2 liters of boiling deionized water,and dried in vacuum at 120°C for 24 hours. The dried cake was grounded and a sieve fraction of the 80 - 100 mesh was taken for all experiments.

(b) Characterization: XRD, TPR and Mössbauer spectroscopy :

X-ray diffraction patterns were obtained by a Toshiba diffractometer using Fe-Kα radiation. Mössbauer spectra were obtained by using a constant acceleration spectrometer with a Co in Pd source. Isomer shifts were reported relative to Fe foil at room temperature, while hyperfine field was calibrated against the 331 kOe field of α-iron. The spectrum obtained was fitted into Lorentzian line shapes by a least square Newton-Gassiun program. The equipment for Mössbauer measurement, multichannel analyzer, driver, and transducer are shown in Fig. 2. Temperature programmed reduction profiles were obtained with a U shaped quartz reactor with 10% hydrogen in argon mixed gas (Fig. 3). Temperature of the reactor was programmed by a Eurtherm type 211 temperature programmer. Concentration of the effluent gas was monitored as function of temperature by thermal conductivity detector in a Shimadzu 3BT gas chromatograph.

(C) Activity test :

Activity test were carried out in a SS-316 stainless steel fixed bed reactor with 3 stage temperature control. The reactor is shown in Fig. 4 and the schematic diagram & the apparatus is shown in Fig. 5. Temperature in the catalyst bed is monitored by a CA thermocouple inside the catalyst bed which can be controlled within ±1°C. Carbon monoxide (Union carbide CP 99%) as purified by passing through molecular sieve 5A at 250°C to remove carbonyls. Hydrogen was purified by passing through a column of Harshaw 0104 Nickel to remove oxygen and then through a bed of molecular sieve 3A to adsorb moisture. The gas product was on line sampled through a heated six port sampling valve, separated by a poropack Q column (4m, 70°C-210°C), and analyzed by two detector in series, one is thermal conductivity detector (Shimadzu GC 8A TCD) to detect CO and CO_2, and the other is flame ionization detector (Shimadzu GC 8A FID) to detect hydrocarbons up to C_9. The liquid product was analyzed by a SE-30 column (2m, RT-250°C). About 3 g of fresh catalyst was loaded and was insitu high (500°C) or low (330°C) temperature reduced or pretreated in a 70 cc/min flowing hydrogen or carbon monoxide. The reaction conditions chosen were 140 psig, 320 °C, and GHSV of approximately 500 cc/g.hr to control the conversion at about 90%. So selectivities can be compared at about the same secondary reaction level. Selectivities and conversions were recorded as a function of time on stream. The used or reduced catalysts were coated with collodion (Merk 4%) in dry nitrogen to prevent oxidation in XRD and Mossbauer spectroscopy measurements.

RESULTS and DISCUSSIONS :

(a) Phase composition of freshly prepared and calcined catalysts:

Figs. 6 and 7 show the Mössbauer spectrum of catalysts before and after calcination. The corresponding computer fitted Mössbauer parameters are summarized in Table 1. Some typical XRD patterns are shown in Figs. 8 and 9. As can see from Fig. 8, the X-ray powder diffraction spectroscopy of 120 °C vacuum dried catalysts have only small and broad peaks, showing samples were poor crystalline. For pure iron and Fe/Mn=9/1, the pattern is - Fe_2O_3 , while for Fe/Mn=1/1, 1/9 and pure manganese, only peaks of γ-Mn_2O_3 are observed.

The Mössbauer spectra of the uncalcined catalysts shown in Fig. 6 is basically composed of two parts, one is a central doublet which is proved to be γ-FeOOH and the other is a broad sextet which can be identified as α-FeOOH. For the sample was only 120 °C vacuum dried for 24 hrs, there is still relatively large amount of water retained. From the study of TGA and DTA, Bearns (4) have found that copreceipatated catalysts can only be completely dehydrated above 250°C, and γ-Mn_2O_3 is formed within 200°C and 280°C. As can be seen in Fig. 6, the sextet is very broad and does not match with usual 3:2:1 peak area ratio. Especially for Fe/Mn=1/1, and 1/9, the internal magnetic field of iron oxide is collapsed or nearly be collapsed due to water retained in the lattice of the oxide or due to imperfect crystallization. Bearns (4) also made an IR test on the copreceipatated sample and reported that no OH stretching

absorbance was observed. Thus, although the Mössbauer spectroscopy of the 120°C vacuum dried sample is very similar to α-FeOOH and γ-FeOOH, a stoichiometric perohydroxide was by no means formed. It is almost certain that the 120°C vacuum dried sample is just hydrated, not well crystallized oxides, which may have a Mössbauer spectroscopy very similar to perohydroxides.

Nevertheless, if we take the indexed hexagonal Miller index of the XRD spectrum of Fe/Mn=9/1 catalyst just described and using the d-spacings calculated from 2 value, the hexagonal unit cell dimension of the observed α-Fe_2O_3 can be obtained by least square fittings. The obtained values of A=4.89 and C=13.44 A are relatively smaller than those appeared of A.S.T.M standard.(A=5.03 A; C=13.75 A) indicating some of the foreign ions must have incorporated into the hematite lattice. Since hematite is the only phase observed, all manganese added must have dissolved into hematite, and a mixed lattice binary oxide $Fe_{2-x}Mn_xO_3$ has been formed. Similarly, the XRD peaks of the γ-Mn_2O_3 phase of Fe/Mn=1/1, and 1/9 can be fitted into a tetragonal lattice, the unit cell dimension obtained are A=5.82 A and C=9.49 A for 1/1, and A=5.76 A and C=9.45 A for 1/9, respectively, all relatively higher than the A.S.T.M standard values; A=5.73 A and C=9.33 A; for pure γ-Mn_2O_3. Thus, since γ-Mn_2O_3 is the only phase detected by XRD, all iron ion must have dissolved into the manganese oxide lattice, and another solid solution $Mn_{2-y}Fe_yO_3$ is therefore formed. Bearns (4) has made similar analysis. From the XRD pattern (Fig.8), we can see that for Fe/Mn=1/9, the peaks of γ-Mn_2O_3 are clearly spaced and almost all the peaks of

manganese oxide can be detected. This sample is better crystallized. But for 1/1, the peaks are rather small and broad and the full spectrum can not be detected. This is probably due to the large amount of iron ions present in the 1/1 sample, they fill in the γ-Mn_2O_3 lattice to make some crystal planes missing and no sharp peak are detected in the XRD pattern.

After vacuum drying, the catalysts were calcined at 500°C in argon for 12 hours. The Mössbauer spectra of the calcined catalysts are shown in Fig. 7. Some representative XRD patterns are shown in Fig. 9. It can be seen that after calcination, the X-ray diffraction peaks became sharp and big, showing the catalysts are well crystalline. For pure iron, the XRD pattern is typical of α-Fe_2O_3 and its Mössbauer spectra shows a clear sixtet and a broad central doublet. The sextet has a magnetic field of 512 koe which can be easily identified as α-Fe_2O_3. The doublet has an isomer shift value characteristic of the high spin Fe^{+3} ion and can be ascribed to very fine crystals of superparamagnetic hematite. For Fe/Mn=9/1 after 500 °C calcination, The XRD pattern still shows that hematite is the only detectable phase, and no peaks of manganese oxide are observed. Its Mössbauer spectra has only a clear sixtet of hyperfine interaction , which is very similar to α- Fe_2O_3 , except that its magnetic field is only 502 koe, considerably smaller than the standard 515 koe value of hematite. This means that manganese ions have incorporated into the hematite lattice and a solid solution $Fe_{2-x}Mn_xO_3$ is formed. Furthermore, if we calculate the unit cell dimensions of the hematite phase using

the XRD data, the A and C values obtained (A=4.97 A; C=13.69 A) are all relatively lower than the A.S.T.M. standard (A=5.035 A; C=13.75 A). Since hematite is the only phase observed by both XRD and Mössbauer spectroscopy, all manganese must have dissolved into iron oxide. The phase of this catalyst after calcination is $Fe_{1.8}\ Mn_{0.2}O_3$, a single phase solid solution.

For Fe/Mn=1/1 calcined at 500°C, both α-Fe_2O_3 and Mn_2O_3 peaks appear in XRD pattern. But the manganese phase has turned from tetragonal γ-Mn_2O_3 to cubic Mn_2O_3. In accordance with Bearn's observation (4), pure manganese oxide is orthorhombic up to 300 K, but slight addition of iron makes it cubic down to 0 K(13). The Mössbauer spectroscopy of the 1/1 catalyst calcined at 500 °C is composed of a clear sixtet and two unresolved doublets. The sixtet is the hematite phase as described above for 9/1, and from its smaller Hf value and smaller hexagonal unit cell dimensions (summarized in table 1) obtained from XRD data, it is believed that some manganese have dissolved in it. The two unresolved doublets are identified as iron ions dissolved in the cubic manganese(III) oxide phase. The solid solution $Mn_{2-y}Fe_yO_3$ has the bixbyte structure (14) with Neel temperature of about 50-70 K (13). At room temperature, its spins are not ordered thus no magnetic splitting is observed in the Mössbauer spectrum. From the phase diagram of the $(Fe,Mn)_2O$ system (15) as shown in Fig.10, it can has a single phase homogeneous solid solution up to y=0.6. Iron can occupy two kinds of nonequivalent sites in the bixbyte structure; one is the less symmetric 24(d) site, which is attributed to the doublet with larger quadrupole

splitting, the other is the more symmetric 8(a) site and corresponds to the smaller quadrupole splitting doublet. The previous study of the Mössbauer spectroscopy of bixbyte (13,16-18), showed that IS(a), IS(d), and QS(d) are almost independent of composition, among which only QS(a) varies with iron content, probably due to different number of manganese ions in the second coordination sphere. Grant (13) has observed that QS(a) increases from 0.526 mm/sec to 1.036 mm/sec as y changes from 0.06 to 0.33. He has also found the site population is distributed according to the Boltzman distribution :

$$\exp(-\Delta/kT) = \frac{y\ (\ 1 + y - 4x\ )}{3 + y\ (\ 3 - 4x\ )}$$

where x is the iron concentration in the formula $(Mn_{1-x}Fe_x)_2O_3$, y = Ad/Aa is the area ratio of the two doublets in the Mössbauer spectrum, Δ is the enthalpy difference between two sites and T is the absolute temperature. According to Grant's data, Δ = 0.08 eV. From our fitted result of the spectroscopy, y = Ad/Aa = 1.71 and using an equilibrium temperature of 773 °K, x may be calculated to be 0.457. The XRD pattern of the manganese oxide phase can be fitted into a cubic lattice, the unit cell dimension obtained is A=9.485 A, which is very close to stoichiometric $(FeMn)O_3$ unit cell distance (13). Thus the amount of iron that has dissolved into manganese oxide is very large, while the amount of manganese dissolved in the hematite is relative small. From the analysis shown above and the relative amount of iron in two phases measured by Mossbauer spectroscopy, a simple mass balance for iron can roughly give the composition

of the two phases as , $(Fe_{0.533}Mn_{0.467})_2O_3$ and $(Mn_{0.543}Fe_{0.457})_2O_3$.

The XRD pattern of the calcined Fe/Mn=1/9 catalyst shows only cubic manganese(III) oxide peaks, no other crystalline phases are observed. Its Mössbauer spectra has only two central doublets, which are the trivalent iron in two nonequivalent sites of the bixbyte structure as described above. Both X-ray and Mössbauer evidence indicate that iron has all dissolved into the manganese oxide to form a single phase solid solution $(Mn_{0.9}Fe_{0.1})_2O_3$. From the phase diagram of Fe,Mn - O system (Fig. 10), composition of iron at mole fraction of 0.1 is indeed in the single phase region up to 870°C. Butt (6) thought that calcination at 500°C may not be enough to equilibrate the system, thus he calcined a 20% iron content catalyst at 1100°C and truly a single phase $(Mn_{0.8}Fe_{0.2})_2O_3$ solid solution was obtained. For our catalyst, iron concentration is only 10%, the temperature of 500°C should be pretty enough to attain equilibrium. The spectrum has a (a) to (d) site area ratio of approximately 1. Using Grant's site distribution equation taking Δ =0.079 eV, x value is calculated to be 0.09 . Cubic unit cell dimension fitted from XRD data is 9.14 A, consistent very well with the published data for x = 0.097. Thus for Fe/Mn=1/9 calcined at 500°C, a single phase solid solution $(Fe_{0.1}Mn_{0.9})_2O_3$ is the only phase existing in the catalyst.

(b) PHASE COMPOSITION OF HIGH AND LOW TEMPERATURE REDUCED CATALYSTS :

Some preliminary reaction tests showed that uncalcined catalysts had better 2-4 carbon olefin selectivity. Therefor the uncalcined catalysts were reduced at high (500°C) and low (330°C) temperature by hydrogen for 12 hours and their XRD and Mössbauer spectroscopy were undertaken to see how the phase changes occur during reduction.

The Mössbauer and some representative XRD spectra for the catalysts reduced at 500°C are shown in Fig. 11 and 12. The fitted parameters and XRD identification as well as the unit cell dimensions calculated are summarized in Table 2. For pure iron, high temperature reduction induces a Mössbauer spectrum of a clear sixtet of α-iron. The absence of other observable phases shows that the catalyst is completely reduced. But for Fe/Mn=9/1, there are still two small doublets beside the sixtet of α-iron. These two doublets are attributed to the spinel $Mn_{3-y}Fe_yO_4$ manganosite and the wustite - Mn(II)O solid solution $Fe_{1-z}Mn_zO$ respectively. The amount of α-iron is only about 89 % of total iron content. This indicates that after only 10% of manganese addition, the whole catalyst can not be completely reduced even at 500° C by hydrogen.

The phase existed can be seen more clearly in the XRD pattern in Fig.12. The XRD results of high temperature reduced Fe/Mn=9/1 catalyst has small peaks of Mn_3O_4 and MnO, but Mössbauer spectra indicates that there exist divalent iron and non magnetically

ordered trivalent iron. Wustite (FeO) is not stable at room temperature, and it can not be seen in XRD pattern. Thus iron(II) must have incorporated with Mn(II) to form a solid solution of $Fe_{1-z}Mn_zO$, and the trivalent non magnetic iron is dissolved in the Mn_3O_4 to form a manganosite spinel solid solution, This can be seen from Table 2 that the unit cell distances calculated all differ from that of the value of A.S.T.M. standard and is consistent with previous studies (4,6, 19-32) and this will be more clearly stated in next paragraphs.

For Fe/Mn=1/1 and 1/9, the 500°C reduced catalysts have Mössbauer spectrum almost identical with that of 9/1, except that the central doublets of the manganosite spinel and wustite phase are increased to a greater extent. Consequently the MnO and Mn_3O_4 peaks in the XRD pattern are also increased.

For catalysts reduced at 330°C, the Mössbauer spectra and the XRD pattern are shown in Fig. 13 and 14, respectively. For pure iron, the spectrum is mainly composed of α - iron, but there exist two small sixtets of the Fe_3O_4 magnetite phase. Magnetite has the spinel structure which is a face center cubic close packing of oxygen ions. There are two kinds of interstices that metal ions can occupy. One is octahedrally coordinated by oxygen and is called the octahedral site, the other is tetrahedrally coordinated and is the tetrahedral site. The two sixtets corresponds to Fe^{+3} in tetrahedral site and one Fe^{+2} and one Fe^{3} in octahedral site, respectively. For there is a fast electron exchange between Fe^{+3} and Fe^{+2} ions in octahedral sites above the Verway transition temperature (about 110 K) (33), one cannot

distinguish the oxidation state of the two ions in octahedral sites from the spectra. Its fitted isomer shift is in between the high spin Fe^{+2} and Fe^{+3} value. From the figure, we can see that degree of reduction is considerably high for pure iron, but on addition of 10% of manganese, as in the Fe/Mn=9/1 case, a drastic change occurs in the Mössbauer spectrum. The spectrum for 330 °C H2 reduced Fe/Mn=9/1 catalyst is mainly composed of the two central doublets, with small sixtets of α-iron and magnetite in the shoulder of doublets peaks. The central doublets is identified as the $Mn_{3-y}Fe_yO_4$ spinel (the doublet with smaller isomer shift) and the $Fe_{1-z}Mn_zO$ (the doublet with larger isomer shift) as stated above. The magnetite phase has hyperfine fields of 486 and 447.8 koe, considerably smaller than standard Hf value 505 and 453 koe for pure magnetite. This is characteristic of mixed lattice spinel $Fe_{3-x}Mn_xO_4$. Some manganese ions must have dissolved in the magnetite to make the internal magnetic field decreased. Analysis of the XRD pattern gives the same clue (See Table 2). It is worthy of notice that the linewidth of the b site iron (1.17 mm/sec) is considerably larger than the natural width, or the width of pure magnetite. The magnetite phases formed must have a wide distribution of composition, Butt (6) has estimated the x value to be in the range of 0 - 1. As for the fully reduced α-iron phase , its magnetic field is 332.4 koe, matches the 331 koe standard value for metallic iron within experimental error. No alloy has ever been formed. Addition of manganese stabilizes the intermediate product such as manganosite spinel and wustite in reduction sequence but in the final stage

of the reduction, phase separation would still occur to form α-iron.

When the manganese concentration is further increased, such as Fe/Mn=1/1 and 1/9, the catalysts can only be reduced to the manganosite spinel and the wustite solid solution by hydrogen at 330 °C, as can be seen from the two unresolved doublets in their Mössbauer spectra. Differences between two catalysts is only the relative amount of the two phase formed. Further evidence came from the X-ray diffraction data. The XRD spectrum of 330°C hydrogen reduced Fe/Mn=1/9 catalyst are shown in Fig. 14, in which we can only observe the peaks of Mn_3O_4 and MnO. Because of the manganosite spinel $Mn_{3-y}Fe_yO_4$ and FeO-MnO solid solution have essentially the same crystal structure with Mn3O4 and MnO, the two phases observed by Mössbauer spectroscopy are exactly the two phases detected by XRD pattern. Bearns (4) identified the formation of $MnFe_2O4$ and found that the wustite phase had incorporate manganese ions by measuring the unit cell distances. Butt (6) found on Mössbauer spectrum the formation of $Mn_{3-y}Fe_yO_4$ manganosite spinel as a Fe+3 doublet. y value varies from 1 to 3. The wusitite divalent iron was also observed by Butt.

The two doublets of the FeO-MnO and the manganosite spinel can be further analyzed to show substructures. Fig.15 shows Mössbauer spectra of the 330°C hydrogen reduced 1/1 and 1/9 catalysts taken on an expanded velocity scale. The Figure shows that the FeO-MnO solid solution phase can be further fitted into 2 doublets with different isomer shift values. There is still no conclusive interpretation for the Mössbauer spectra of the wusitite phase

from the collected literature (31-33). But according to Elias (34), there is no stoichiometric FeO compound without cation deficiencies. There must be some ferric iron ion existing in the tetrahedral site of the face center cubic oxygen lattice, and a fast electron exchange between divalent and trivalent ions happens to make the isomer shift deviate from its high spin Fe^{+2} value. One doublet corresponds to ferric and ferrous iron in octahedral sites involving electron exchange while the other doublet is the ferric iron in tetrahedral sites having electron exchange with neighboring ferrous iron. For catalyst 1/9, two doublets has almost the same isomer shift and the value of isomer shift are exactly characteristic of divalent iron, thus the iron ion in this sample are about all in divalent state. Previous study about (Fe,Mg)O has pointed out that a stoichiometric compound can be made (30), and a single doublet can describe the spectrum. For our sample, a single doublet can also give a satisfactory fit. Furthermore, XRD evidence showed that it is a manganese(II) oxide pattern, it is iron that dissolved into manganese(II) oxide, and the sample formed is rather like MnO but not $Fe_{1-x}O$. A stoichiometric compound $Mn_{1-x}Fe_xO$ may have been formed. All iron and manganese ions might be all in octahedral sites and the whole crystal is simple cubic rock salt structure with no cation deficiencies. But for catalyst Fe/Mn=1/1, (Fig. 15) the two doublets has different isomer shifts, one is characteristic of Fe(II), and the other is in between the trivalent and the divalent oxidation state. Some Fe^{+3} must exist in this phase and the compound is rather wusitite like although

we cannot find its x value. The fitted Mössbauer parameters were listed in Table 3.

For the manganosite $Mn_{3-y}Fe_yO_4$ phase, the spectrum taken on a expanded velocity scale (Fig.15) can also be fitted into two doublets with different quadrupole splittings. According to Bornaz and Singh (25,29), manganese(III) is a Jahn - Teller ion, its d orbital is severely tetragonal distorted, and may cause a strong electric field gradient in the lattice. The doublet with larger quadrupole splitting is then attributed to the iron ion that its second coordination sphere has some manganese in it, and the doublet with smaller quadrupole splitting should correspond to the iron ion that is totally surrounded by iron. For sample 1/9, the larger quadrupole splitting doublet is rather small while in the 1/1 case it has a large fraction of the larger quadrupole splitting doublet. Thus iron in the manganosite spinel may not be randomly distributed according to total iron content, but they may choose its favorest sites according to the symmetry of the lattice. The exact picture needs further inside study.

(c) TEMPERATURE PROGRAMMED REDUCTION STUDY :

Besides the studies of X-ray diffraction and the Mössbauer spectroscopy a set of temperature programmed reduction experiments were undertaken. Five different kind of catalysts prepared were tested in a TPR cell after different pretreatments, such as without calcination , calcined in an inert gas (argon), and calcined in air at 500°C for 12 hours. The TPR spectra obtained are shown in Fig. 16 to 18. For pure iron , the spectrum

has a small peak at about 300°C and a huge peak at 550°C , the small peak corresponds to the reduction of Fe_2O_3 to Fe_3O_4, and the big peak at higher temperature is ascribed to the reduction of magnetite to metallic iron (35). For pure manganese oxide, there is only a single peak at about 400°C, which is due to the reduction of cubic Mn_2O_3 to manganese (II) oxide. The reduction of manganese can take place before iron can be totally reduced. For binary oxides, as can be seen from the Figure, the peak due to reduction of Fe(III) to Fe(II) gradually disappears while the peak due to reduction of manganese increase its size as the manganese content is increased. In the middle part of the spectrum for the binary oxide catalysts, the peaks became flatten and broadened. This means the formation of mixed lattice oxide of variable compositions. Reduction take place via changes of the x, y, and z, values and a clear, definite stoichiometric chemical reaction equation of reduction cannot be written.

For the uncalcined catalysts, the TPR patterns have a lot of trisidual peaks because they undergo dehydration and crystal phase changes along with reduction. For catalysts calcined in air, there is another peak before the reduction of manganese (III) to manganese (II), which may be the reduction of Mn (IV) to Mn (III), tetravalent manganese may be produced during the calcination in an oxidizing atmosphere.

Summarizing the results of Mossbauer spectra, XRD, and TPR, it can be concluded that the addition of manganese prohibits the reduction of the catalysts. Iron cannot be completely reduced on addition only 10% of manganese even by hydrogen at 500°C. The

peaks of the TPR of manganese containing catalysts become broad and its temperature shifts towards central part of the spectrum. The wusitite phase detected by Mössbauer and XRD is not stable at room temperature, but stabilized by incorporation of some manganese in it (5). Addition of manganese as a matter of fact stabilizes the intermediate phases of reduction and thus prohibits the total reduction of the catalysts. This can be seen even more clearly when examined the catalysts after synthesis for which oxidation has occurred. The whole reduction scheme may be speculated as to proceed via the following steps :

$$Fe_{2-x}Mn_xO_3 \longrightarrow Fe_{3-x}{}'Mn_x{}'O_4 \longrightarrow Fe_{1-x}{}''Mn_x{}''O \longrightarrow Fe + MnO$$

$$Mn_{2-y}Fe_yO_3 \longrightarrow Mn_{3-y}{}'Fe_y{}'O_4 \longrightarrow Mn_{1-y}{}''Fe_y{}''O \longrightarrow Fe + MnO$$

x and y values change continuously during reduction, thus the final composition is drastically complicated and severely depends on reduction temperature. This is also the reason why that various investigators used different pretreatment conditions and different results was obtained. Different reducing temperature or different bulk composition can lead to totally different phase structure. Thus different catalytic behavior is observed.

(D) PHASE COMPOSITION OF CATALYSTS AFTER REACTION :

Because pure manganese was proved to process no activity, the other four different catalysts were subjected to a Fisher Tropsch synthesis after they were reduced in situ at high (500 C) and low (330 C) temperatures respectively. The reaction conditions chosen

are 320°C, CO/H_2=1, 150 psig and GHSV of approximately 500. After about 50-150 hours activity test, the catalysts were taken out in an inert gas (N_2) atmosphere and coated with collodion (4) in order to prevent oxidation in air. The Mössbauer spectra obtained are shown in Fig. 19 and 21 with parameters summarized in Table 4. Some XRD patterns are presented Figs. 20 and 22. Fig. 19 shows the Mössbauer spectra of the used catalysts reduced at 500 °C. For pure iron, it is mainly composed of 3 sixtet of X-Fe_5C_2 carbide. But in the rear of the spectra, it can be clearly seen that there exists 2 sixtets of magnetite, amounts about up to 16% of the total spectra area. Referring to the last section we know that pure iron is totally reduced to α-iron after 500 °C hydrogen reduction. Thus some oxidation must have occurred along with carburization. It probably is due to the carbon dioxide and water formed in synthesis that make gas phase oxidative. In a 90% conversion level, the effluent gas from the reactor can contain a carbon dioxide concentration as high as 50% for 1/1 CO/H2 feed. Carbon dioxide is mainly produced via water shift reaction, and water gas shift reaction is proceed via a oxidation reduction cycle mechanism (36), thus there must be some oxidized phases to be in equilibrium with the surrounding gas. This is in contrast with differential reactor studies which all gas phase remains reductive throughout the whole bed. Satterfield (37) studied a fused iron catalyst using slurry reactor and found that the catalyst contained certain amount of magnetite after synthesis. Rymond et al (38) also reported that Fe_3O_4 along with carbides can be observed by XRD using a pure iron catalyst

obtained by thermal decomposition of nitrate salt.

For Fe/Mn=9/1, the used catalyst also contains about 16% of magnetite after synthesis, the rest of the phases is mainly X-carbide. But in the central part of the spectrum, there has to be added 2 doublets to full fill the fit. These doublets are the wusitite-manganese(II) oxide and the manganosite spinel as found in the 500 °C hydrogen reduced catalyst. Their spectro area amounts up to 11% of the total iron content. But it is only 5% in the freshly reduced state, Thus oxidation of the catalyst must be through these two phases as described in the reduction scheme, but only now it is a reverse path. For this catalyst is only reacted for 20 hrs, there is still certain amount of α-iron exists after synthesis. The oxidation reduction trend can be seen even more clearly in the 330°C reduced catalyst, which will be described in detail in later paragraphs. For Fe/Mn=1/1, the used catalyst shows a completely different Mossbauer spectrum as can be seen in Fig. 19. The phases present in the Figure are mainly iron manganosite spinel and the wusitite manganese (II) oxide solid solution, there is still a little amount of Fe_3O_4 solid solution and carbide phase exists. But it only amounts to about 3% of the total spectroscopic area. As can be speculated from the present results, the oxidation of the catalyst is more clearly seen in the Fe/Mn=1/1 catalyst, for there is a larger amount of manganese, the lower oxidation state intermediate phase of reduction - oxidation trend, the manganosite spinel and wusitite phase is stabilized. thus the phases present in the used catalyst is the less oxidized phase as observed ir TPR results compared to

pure iron and 9/1 catalyst. More surprisingly, the carbide in this catalyst is turned from X-Fe_5C_2 to ε'-$Fe_{2.2}C$, for the amount of carbide is very small, it is probably on the surface. This is in connection with the catalytic behavior of this catalyst, and will be discussed later.

For Fe/Mn=1/9, the used catalyst can find no magnetite in it, but instead the catalyst is mainly composed of wusitite solid solution and the manganosite spinel, as can be seen from Fig.19. Proved on further addition of manganese, the less oxidized phases is even more stabilized. For this catalyst is reduced at 550 °C instead of 500 °C, considerable amount of α-Fe is formed in reduction step, thus there is a large amount of X - $Fe_{2.5}C$ carbide present in the catalyst. On looking upon the whole oxidation carburization trend during synthesis, addition of manganese to iron catalyst has the effect of stabilizing the oxidized phase via formation of mixed oxide solid solution, which will affect the catalytic behavior of the catalyst. This will be discussed in detail in the results of activity test part. The XRD pattern also shows the formation of X-Fe_5C_2 carbide, magnetite, Mn_3O_4, and FeO-MnO solid solution for the used catalysts reduced at high temperature as discussed above, but there is no carbides observed by XRD for high manganese catalysts such as 1/1 and 1/9. Carbides are usually not well crystallized as oxides, and most of the evidences existed come from Mössbauer spectroscopy.(39-45).

For the low temperature (330°C,H2) reduced catalysts, the Mössbauer spectra of the samples after 150 psig 320°C CO/H_2 Fisher Tropsch synthesis are shown in Fig. 21. There are three

catalysts tested; pure iron, Fe/Mn=9/1, and Fe/Mn=1/9. For pure iron, the phases existed after synthesis are still X-Fe_5C_2 carbide and magnetite, but the amount of magnetite is increased from 16% to 46% as comparing the high and low temperature reduction cases. Pure iron catalyst has already about 14% of magnetite after 330 °C hydrogen reduction as described in last section. Oxidation during synthesis must proceed to further extent thus the magnetite phase grows to a greater amount. But for there is no manganese in the sample, the wusitite phase is not stable in the present condition used. Therefor it has no divalent oxide observed in this catalyst. Because the catalyst is over 80% reduced before synthesis, the carbide is easily formed.

For catalyst Fe/Mn=9/1, the Mossbauer spectra of used sample shows a completely different characteristic with the freshly reduced one. Sample reduced at 330°C in hydrogen is composed of over 65% of wusitite and manganosite spinel, plus some alpha iron and magnetite. After synthesis, it is turned to 30% of X-Fe5C2 carbide, 60% of magnetite, and about 10% of the wusitite and manganosite spinel. It has been oxidized to higher oxidation state. For this catalyst, there is only 10% of manganese present in the sample, the amount of manganese is not large enough to stabilize the lower oxidation state of the catalyst in the present reducing and synthesis condition used. Iron and manganese in the wusitite and manganosite spinel phases must have separated during reaction in freshly reduced Fe/Mn=9/1 catalyst. For Fe/Mn= 1/9, as can be seen from Fig.21 the used catalyst is relatively unchanged as compared to the reduced one. Large amount of

manganese has stabilized the intermediate phases in oxidation reduction scheme and the catalyst can remain in the wusitite and manganosite stage even in a oxidative environment. But on comparing the relative amount of the two phases before and after synthesis, it still can be found that higher oxidation state phase, the manganosite, is increased to a greater extent .Some oxidation still occurs. Besides these two phases, there is some carbide in this catalyst after synthesis. From one sextet and unique internal field, it is identified as ε'- $Fe_{2.2}C$. Therefor lowering down the reduction temperature and increasing manganese content may change the carbide formed from X-Fe_5C_2 to ε'- carbide. ε'-carbide is less stable than X-Fe_5C_2 carbide no matter in higher temperature or in higher hydrogen partial pressure.(39) According to Delgass (40) and J.B Butt (41), ε'- $Fe_{2.2}C$ carbide can be formed by a smaller particle size iron catalyst supported on silica. We are not certain whether this carbide formation is totally a particle size effect due to lower iron content or is some chemical effect caused by manganese. But the addition of larger amount of manganese can certainly affect the form of carbide formed. And this has a drastic effect on the catalytic test results as will be discussed in detail in the next section.

Unlike θ-Fe_3C or X-$Fe_{2.5}C$, ε'-$Fe_{2.2}C$ cannot be exactly sure as an stoichiometric carbide, and so far there is still no exact crystallographic determination of the structure of these carbides (39). Because the particle size of this carbide formed in synthesis is very small, and very difficult to detect by XRD, the XRD pattern of the 330°C reduced Fe/Mn=1/9 catalyst had only

peaks of MnO and Mn_3O_4, No ε'-$Fe_{2.2}C$ carbide is observed.

(E) CO HYDROGENATION WITH HIGH AND LOW TEMPERATURE HYDROGEN REDUCED CATALYSTS :

After reduced in hydrogen at high (500°C) and low (330 °C) temperature in situ respectively, a activity test is done on four kinds of catalysts prepared. The reaction conditions were as previously described. Results recorded as a function of time on stream are, presented in Figs. 22 and 23.

For 500°C reduced catalysts, pure iron and Fe/Mn=9/1 reach their maximum conversion level after about 5 hrs on stream, as can be seen in Fig.22, and gradually decrease afterwards. While for Fe/Mn=1/1 and Fe/Mn=1/9, the activity increases with time, and kept on increasing even after 80 hrs reaction, showing a completely different trend. For low temperature reduced catalysts, however, all catalysts seem to be able to maintain a stable activity after 10 hrs on stream. Bearns (5) has also observed the activity vs. time pattern even on a longer testing time. As for selectivity, as shown in Fig.23, the high temperature reduced Fe/Mn=1/1 catalyst has the highest 2-4 low carbon olefin yield, which is about 38% of total hydrocarbon produced. It also has the highest C5+ heavy product selectivity, which is about 40% of the total hydrocarbon. Thus the 1/1 catalyst has the most pronouncing promoter effect on addition of manganese after high temperature reduction. For the low

temperature reduced catalysts, the selectivity pattern deviates to less extent as compared to high temperature reduced ones. But it still can be seen from Fig.23 that the high manganese containing catalyst, Fe/Mn=1/9, has the highest 2-4 low carbon olefin and C5+ high molecular weight hydrocarbon producing ability. Another fact worth of notice is low temperature reduction seems to be able to lower down methane selectivity. High temperature reduced catalysts has maximum methane selectivity of about 30%, which is created by pure iron after 80 hrs on stream. While for low temperature reduced ones, it is only about 20%, still made by pure iron. Paraffin also has the same trend, high temperature reduced catalysts has a max. 2-4 carbon paraffin of about 55% and decreasing to a steady value of 35%, still higher than low temperature reduced ones. Addition of manganese or lowering down reduction temperature seems to be able to lower down the ability of hydrogenation. This can be correlated with oxidation state of catalysts and will be discussed in detail in discussion section. Comparing with the phase identification result described in the last section, we can see both catalyst Fe/Mn=1/1 reduced at high temperature and Fe/Mn=1/9 reduced at low temperature have the most significant promotion phenomena. They have a common characteristic that their crystalline phases after synthesis are all composed of wusitite - manganese(II) oxide solid solution and the iron manganosite spinel. Boeyens (42) in a newest report has claimed that the wusitite and manganosite spinel is the phases that is responsible for high olefin production. This is further proved here. As for carbide formation, there is no direct evidence that the more

unstable ε'- $Fe_{2.2}C$ carbide has the effect on selectivity. But ε'- $Fe_{2.2}C$ carbide can be formed in a small particle size alpha-iron precusors (40,41). Basset (43) has created very small iron particles on alumina oxide support by decomposition of iron carbonyls and observed by Mossbauer spectroscopy as a super-paramagnetitic singlet of alpha iron. Particle size is smaller than 3nm. Indeed, very high 2-3 carbon olefin selectivity is resulted although iron particles sinter very fast during reaction and it is only a differential reactor data. Thus it is speculated that ε'- $Fe_{2.2}C$ carbide can affect the form of surface active carbon formed and therefore affects the selectivity. This will be discussed in detail in discussion section where a model will be proposed to sum up all evidence collected.

Another interesting phenomena worth of notice is the 2-4 carbon paraffin selectivity vs. time pattern. For all the catalytic testing run, there all existed a common trend that the 2-4 carbon paraffins yield decreases with increasing time on stream. Methane has a stable selectivity through out the whole run, except for pure iron which is increased gradually as activity dropped. The 2-4 carbon olefin and heavy products increase with time on stream. This of course the phase changes occur has important responsibility for it, and the hydrogen remaining on the surface after in situ reduction has some pronouncing effect. As can be seen from the figure the methane selectivity is always very high in the first 1-2 hours, but it turns to a normal selectivity value very fast after about 2 hrs on stream. This

indicates that hydrogen left on surface after reduction has no effect on long term time dependency. Summing up the above mentioned evidences, carbon monoxide seems to have some effect of carburizing the more hydrogenation active phases like pure iron thus poisoning the hydrogenation site to enhance the olefin production. As can be observed in figure that paraffin decreases while olefin increased with time on stream. Kolbel (3) in his published patent also used a carbon monoxide pretreating procedure from which very high olefin producing ability was obtained. Therefor the effect of CO pretreatment on the poison of hydrogenating site must be ascertained. In order to get more inside into the picture, a series of carbon monoxide pretreating effect experiment were also done. The results are presented in the last section.

(F) ACTIVITY AND PHASE COMPOSITION OF CARBON MONOXIDE PRETREATED CATALYSTS

Carbon monoxide pretreatment experiments were done following Kolbel (3). The catalysts tested were pretreated with carbon monoxide and hydrogen successively at the same pre selected temperature for 12 hours, and then the temperature of the reactor was adjusted to reaction temperature in flowing hydrogen. Pre mixed CO/H2=1/1 syngas was fed in, and the activity and selectivity data were monitored by an on line GC as a function of time on stream. After CO hydrogenation, Mossbauer spectroscopy and X-ray diffraction of the used catalysts were undertaken to see the phase changes. The results are shown in Figs. 24 - 27.

Mossbauer parameters and XRD identification are summarized in Table 5 .

There are all two pretreatment temperatures tested, 330 °C and 270 °C. For 330°C pretreated case, pure iron has a severe carbon deposition during CO pretreatment. Because the pressure drop across the catalyst bed exceeds 50 psi no activity test can be done. The other three catalysts are tested. As for 270 °C pretreated case, only the two catalysts showing higher olefin producing ability after hydrogen activation,(Fe/Mn=1/1; and Fe/Mn=1/9) are tested. Reaction condition is chosen the same as used in the hydrogen reduction case, 320 °C, 150 psig, and GHSV of approximately 500. A maximum carbon monoxide conversion over 95% can be reached.

For both 270 and 330 °C CO/H2 pretreated catalysts, activity vs. time pattern are shown in Fig. 24, As can be seen from the Figure, conversion can reach a steady state value after about 5 - 10 hours on stream, and in contrast to the high temperature reduction case, their activity are almost unchanged after steady state is reached. This is very similar to the low temperature hydrogen reduced catalysts. Thus an oxide matrix indeed has the effect of keeping a stable activity. This effect has also been observed by Bearns (5).

As for selectivity shown in Fig.25 ,catalyst Fe/Mn=1/1 shows maximum 2-4 low carbon olefin and high molecular weight product selectivity in the 330°C pretreated case. But the 2-4 carbon olefin selectivity decreases with time for both catalysts

Fe/Mn=1/1 and the Fe/Mn=1/9 pretreated in 330 °C. While their 2-4 carbon paraffin yield increases with time, which is the direct contrary compared to hydrogen reduced catalysts. Therefore some changes must have happened during CO pretreatment. For two catalysts pretreated at 270 °C and reacted at 320 °C, Fe/Mn=1/9 processed higher olefin producing ability, up to 43% of the total hydrocarbon in a about 80% conversion level, this is the highest olefin selectivity we have ever obtained in the whole project. Exactly coincide with Kolbel's results. Thus carbon monoxide pretreatment indeed has it's unique effect. Other informations can be obtained from the activity data is the methane selectivity, here, like in the hydrogen activated case, lower temperature pretreated catalysts, (270 °C) can have lower methane yield. Paraffin dropped in the beginning of the test, but when the hydrogen adsorbed in the insitu activation had been expelled from the catalysts surface, it slightly increases.

The Mössbauer spectrum of the used catalysts are shown in Figs. 26 and 27. The 330°C pretreated catalyst Fe/Mn=9/1, which is only reacted for 5 hours on stream shows two sextet of almost pure magnetite and one doublets which can be attributed to wusitite phase. No carbides are detected. Oxidation seems to occur before carburization. For this catalyst is only reacted for 5 hours, the picture seems not so clear. For catalyst Fe/Mn=1/1 reacted for over 100 hours, a complicated spectroscopy is resulted. Two sextet of magnetite, three sextets of X - Fe_5C_2 carbide, and two doublets of the manganosite spinel and wusitite can give a exact fit. Comparing with hydrogen reduced case, high

temperature H_2 reduced catalyst Fe/Mn=1/1 is composed mainly of iron manganosite spinel and wusitite phase with some ε'- $Fe_{2.2}C$ carbide after reaction. Their olefin selectivity increases with time on stream and can reach a steady state value. But after CO pretreatment it is oxidized to further extent after reaction and the olefin yield also drops. Therefore for catalyst Fe/Mn=1/1 higher reduction temperature has to be used to make the catalyst exist in the desired oxidation state; the wusitite - MnO solid solution and manganosite spinel phase to produce more olefin. The carbide formed may have something to do with CO pretreatment, and this will be discussed later. However, 1/1 still produces more olefin after 330°C CO/H2 pretreatment. For catalyst Fe/Mn=1/9 pretreated at 330°C, Mossbauer spectroscopy is almost about the same with the 330°C hydrogen reduced one. Catalyst is mainly composed of manganosite spinel and the wusitite after reaction for its huge amount of manganese present in the sample. But olefin selectivity is still about the same with low temperature H_2 reduced one. Maximum olefin production occurs in 270°C pretreated case. Looking upon the two used samples pretreated at 270 °C, Fe/Mn=1/9 is still composed of wusitite and the manganosite spinel and ε'-$Fe_{2.2}C$ carbide, only now the amount of carbides is larger. As for catalyst Fe/Mn=1/1, the used sample shows another different kind of spectroscopy, it is composed of some large amount of magnetite, wustite and manganosite spinel, and most surprisingly, the carbide phase has turned from X-Fe_5C_2 to more unstable ε'-$Fe_{2.2}C$. Lower temperature reduction not only make catalyst to oxidize to higher oxidation state, it also changes the carbide formed. To produce more olefin the catalyst

must be properly oxidized to suitable phases as well as to be properly carburized. Oxidation and carburization both play a important role in determining the selectivity. The catalysts Fe/Mn=1/9 pretreated at 270 and 330°C have about the same bulk phases composition, but the olefin yield is almost doubled in the low temperature pretreated catalyst. Summarizing above mentioned evidences, although a little bit diverse, one may still conclude that the higher olefin producing phases, the wustite and the iron manganosite spinel, grow as the content of manganese in the sample increases or as activation temperature decreases. Moreover, as comparing catalyst Fe/Mn=1/1 pretreated at two different temperatures, one may find as the temperature of the pretreatment, not the reaction temperature, is increased, the carbide formed will turn from less stable ε'-$Fe_{2.2}C$ carbide to a more stable X-Fe_5C2 carbide. A complete trend for the factors that influenced the phases formed can be summarized in the following scheme :

Reduction or pretreatment temperature increases ------

------ manganese content increases

------ high oxidation state oxide phases increases

With CO pretreatment ---------

More stable carbide X-Fe_5C_2 increases --------

--------- olefin or heavy hydrocarbon product increases

Although the maximum yield for each catalyst may be different, but one still can obtain its max. yield by adjusting

pretreatment condition used, and the effect seems to be much larger than other kinds of catalysts. Pretreatments indeed play a very important role in determining the catalytic behavior of the iron manganese catalysts.

DISCUSSION :

Following the results presented in the last section, it has been shown that iron manganese catalysts can have various kinds of phases composition of different pretreatment condition are used. During CO hydrogenation, oxidation and carburization occur simultaneously, but gas phase composition depends on conversion level studied. Van Dijk (12) used high temperature reduction and a high H_2/CO (10/1) feed ratio to study the CO hydrogenation within a differential reactor. Their Mossbauer spectrums are exactly the same as our Fe/Mn=1/1 sample calcined and reduced at 500 °C. They interpreted the data as superparamagnetic iron oxide and did not consider the formation of binary oxides. It has been found by many researchers (37,38) that precipitated or fused iron catalysts after CO hydrogenation has a Fe_3O_4 basis besides carbides. We speculated that oxidation should be much correlated with the water gas shift reaction taken place in the reactor. In our tests, the effluent gas out of the reactor is about half of carbon dioxide and half of hydrocarbons, and no water is detected. All oxygens leave as carbon dioxide. Thus a high degree of water gas shift reaction must take place if water is taken as the primary product, otherwise the 50% hydrogen input would not be enough to produce a 90% conversion hydrocarbons. One

of the catalysts used industrially for water gas shift reaction is iron based Fe_3O_4, and recently it has been indicated by Varma (44) that manganese based catalysts may process considerable water gas shift activity. Newsome (36) has reviewed the water gas shift reaction and pointed out that one of the mechanism proposed by Temkin (45) is the oxidation reduction cycle of the catalyst surface. Thus if water gas shift reaction can proceed to some extent in the reactor, the catalyst must be somehow oxidized in order to be in equilibrium with the gas phase. This is very possible the reason why oxidation takes place. Satterfield (46) has studied the effect of water vapor in syn gas feed and found the oxidation of the catalyst increased while carburization decreased along with an increased extent of water gas shift reaction.

The conventional promoters used for Fisher-Tropsch synthesis is alkali metal oxide. Recently it has been reported that some irreducible metal oxide supports, such as titania, alumina, and magnesia, can have a strong interaction with the metal loaded (47,48), which is the well known SMSI effect. Some evidences have shown that titanium has been reduced to a lower oxidation state (49-51). Iron and manganese can form various kinds of binary oxide and spinel solid solutions. It has been reported that their hydrogen and carbon monoxide adsorptions are very low. Mossotch (7,8) studied the Fe-Mn catalysts with IR spectroscopy and found that there is a broad absorption band around 1500 cm. Ichikawa reported that CO on Rh - Mn catalyst has a IR band of 1530 cm (53). These kinds of CO adsorption can remarkably

enhance the dissociation of carbon monoxide and CO insertion. Both reaction is important in olefin and heavy products formation. Further more, it is well known that hydrogen adsorption takes at least a dual metal site to proceed the dissociative adsorption. But in iron manganese bimetallic catalysts, the final form of the catalyst is composed of the wusitite and the manganosite spinel is presumed to be the olefin producing phases. Iron atoms must be somehow separated in these phases as compared to metallic iron. Thus hydrogen adsorption is naturally suppressed. But this is not the case for carbon monoxide, for CO can be adsorbed with carbon attached to iron and oxygen attached to neighboring manganese (52). In this special titled form of adsorption (Fig.28), carbon and oxygen atoms are both activated therefore CO dissociation becomes extremely easy. The wusitite and the manganosite spinel can produce more olefin and high molecular weight hydrocarbons. In a newest report (38), Boeyens has proposed that wusitite and the manganosite spinel is indeed the phases that has the most significant promoter effect. Here, we have further confirmed this discovery, and give a comprehensive explanation on how manganese can stabilize these two phases during the activation and reaction periods.

Van Der Kraan (55) has stated that there are three models to account for the mechanism of CO hydrogenation: the carbide model, the competition model and the slow activation model. Slow activation model can be eliminated for it cannot explain most of the experimental phenomena. But there is still some doubts about the carbide and the competition model. The activity increases almost linearly with the extent of carburization, but alloys and

nitrides of iron, which have an arrays of iron atoms that cannot be carburized, show an immediate activity upon contacting with the synthesis gas. The surface active carbon, the dominating active center in competition model, is still not structurally well characterized. It is often termed as " carbidic carbon " to infer that it is a surface carbide, or sometimes just a " surface active carbon ". In our experiments, we found that the carbide structure formed is highly dependent on manganese amount and the reduction temperature. Higher manganese catalysts reduced in lower temperatures can lead to a more unstable ε'- $Fe_{2.2}C$ while in lower manganese content or higher temperature reduced catalyst, more stable X-Fe_5C_2 was formed. In a recent experiment we have conducted the CO hydrogenation on copper iron spinel catalyst . The results showed that if higher hydrogen partial pressure, $CO/H_2=1/3$, were used, an even more stable carbide, θ - Fe_3C cemmantite was formed. The stability of carbides decreases in the manner: θ- Fe_3C > X - $Fe_{2.5}C$ > ε'- $Fe_{2.2}C$ > Fe_2C > Fe_xC ($x < 2$) (39). Higher temperature or higher hydrogen partial pressure will shift the carbide to more a stable form, for only more stable carbides can exist in a more severe condition. The iron atoms at catalysts surface, they are in direct contact with the hydrogen in gas phase, the carbides at the surface must be in some relatively unstable form. As a matter of fact, the so called surface active carbon may just be the surface unstable carbides. As we can see from the above stability sequence, more stable carbide has a higher Fe to C ratio, but imagine a fresh α- iron just begin to be carburized, the carbides initially formed must

be the most unstable, or the most active. It will undergo some phase changes until finally some relatively stable carbide, -Fe C , was formed. Surface active carbon is in fact a surface unstable carbide. Hydrogenation of surface carbides proceeds via the phase change cycle. In regards to the bulk phases, for it can not be in contact with the gas phase hydrogen, it must go through some phase change at the present temperature to a more stable carbide. Upon the phase change, the excess carbon must combine with each other and forms an inert graphitic carbon, which will block the active site or the pore structure of the catalyst, and leads to the lowering of the activity of the catalyst. If we can take the picture this way, the carbide model and the competition model can be combined together and the time dependency of activity can be satisfactorily explained. But it has to be stated clear that the activity versus time pattern is dependent on the conversion level, for a differential reactor, gas phase composition in reactor is almost unchanged from the inlet to the outlet, and the hydrogen partial pressure remains high throughout the reactor. Thus phase changes of carbides is fast and activities can reach a relatively high level and then falls. But for an integral, low hydrogen feed reactor, hydrogen is consumed in the middle part of the reactor, and carburization happens along with oxidation. They both play an important role in determine the catalytic behavior in iron - manganese catalysts case.

From the above discussion, one important speculation can be drawn. That is, iron catalysts has to be carburized first before carbon deposition. This has been indicated by many authors who

have studied the time dependent behavior of iron catalysts (56 - 59). We also have observed this experimental phenomena. For pure iron or high temperature hydrogen reduced Fe/Mn=9/1 catalysts, the carburization took place, and the activity increased with time on stream and then decreased. But for high manganese catalysts reduced at low temperature, the matrix of the bulk catalyst structure is the oxide structure. There is no metallic iron for carbon to diffuse in and therefore no carbides had ever been formed. There must be some surface carbide which is responsible for the activity, but the amount is too small compared to the bulk phase. Carbon monoxide pretreatment may have played an important role in the surface composition construction. For a catalyst to maintain a stable activity at a high conversion level by using a low CO/H_2 inlet ratio, carburization hydrogenation cycle as well as oxidation reduction cycle for the water gas shift reaction has to be bi-functionally facilitated. Oxides along with carbides must be both on surface. As the manganese in iron catalysts can stabilize the intermediate oxidation state of iron, the oxidation reduction is naturally full filled. As CO is adsorbed via the formation of M - C - O - M' bond on surface, the dissociation of carbon monoxide can be enhanced and surface carbide enriched. With suppressing hydrogen adsorption ability, the olefin producing is therefore increased. There must exist an optimum pretreatment procedure to produce the desired olefin producing phases. From the experimental evidences up to now, these phases are the wusitite - Mn(II)O solid solution and the manganosite spinel. CO pretreatment must be in connection

with constructing the proper surface carbide structure, or to poison the hydrogenating site formed by several iron atom clusters. The high manganese catalysts, Fe/Mn=1/1 and Fe/Mn=1/9, have a different time dependent activity behavior upon high temperature hydrogen reduction. The activity increased very slowly with time on stream. The freshly reduced metallic iron is not very active, but when the wusitite and the manganosite spinel is formed after carburization, the activity increases .

The iron manganese catalyst can exist on various kinds of crystalline phases upon activation, and thus the different catalytic behavior are observed. But inspite of the determination of the bulk structure. The surface construction still is the dominate part to determine the catalytic behavior, especially in CO pretreatment part. Accordingly, some surface sensitive instrument has to be used insitu to see a more clear picture, in order to understand all the hypothesis proposed.

SUGGESTIONS ON FURTHER STUDIES :

Iron catalysts used in Fisher Tropsch is most complicated in the VIII group transition metal catalysts, for it can form various kinds of compounds with carbon. It has been well investigated in the last decade, during energy crises duration. But consulting the existed literature data, previous studies mostly concentrated on supported catalysts, and almost are differential reactor data. But industrially used iron catalysts, no matter it is used for Fisher Tropsch synthesis or other reaction, seldom supported iron catalysts were used for its cheap

price. For Fisher Tropsch reaction, it was even proposed that supported iron did not give a good result. (60) In our labt., Mossbauer technique has been well established but it is still difficult to probe too small a loading or a very small particle size of iron particles. For it mostly give a superparamagnetic doublet that makes identification very difficult. Most of all, most of the industrially used unsupported iron catalysts that its structure or bulk phases is worth of investigation. Take the Fisher Tropsch synthesis as an example, there is still very little experimental data which is high conversion, industrially compatible and well investigated by modern techniques up to now. One more limitation about the supported catalysts is our X-ray diffraction usually can not detect too small a particle of iron, that makes identification of structures soly depends on Mossbauer spectroscopy, thus being short of independent evidences. Therefore, as a personal suggestion, we should do some study about the unsupported iron, collecting data in a high conversion level using high pressure reactor, which will be the unexplored part of Fisher Tropsch reaction and also fit in requirements of our equipments.

We have built up the ability of analyzing a complex Mossbauer spectroscopy and learned a lot of structure knowledge about the spinel or binary oxides. Iron can form various kinds of binary oxides or spinel with transition metals or other elements, a lot of them is catalytically active for various reactions. With our present knowledge or technique, it is not difficult to study these reactions, therefore another direction of research seems

worth of explore.

For iron - manganese system, in Fisher Tropsch reaction, water gas shift reaction plays a very important role as can be seen in the report. Adsorption experiment of hydrogen and carbon monoxide can give a direct picture about the SMSI and its relation with promoter effect. Therefore next step to do I personally proposing is to study adsorption, add water in syngas feed and independently study water gas shift reaction, which can be done kinetically. Professor I. K. Wang has used steam to regenerate their iron catalysts and a very high olefin production resulted. This can also be investigated simultaneously but with sensitive structure probe experimental device like Mossbauer spectroscopy. For iron - manganese catalysts can have a lot of intermediate oxidation state it must be reactive to some surface oxidation - reduction mechanism reactions, like partial oxidation or oxidative dehydrogenation, this is another future direction of research.

REFERENCES :

(1) B. Bussemier, C.D. Frohning and B. Cornils, " Hydrocarbon Processing " 11, 105 (1976)

(2) B. Bussemier, C.D Frohning, G. Horn and W. Kluy, " Deutche Dffenlegungsschrift ", 2518964 (1976)

(3) H. Kolbel amd K.D. Tillmrtz, U.S. patent 4177203 (1979)

(4) G.C. Maiti, R. Malessa and M. Bearns, Applied Catalysis, 5, 151 (1983)

(5) G.C. Maiti, R. Malessa, U. Lochner, H. Rapp and M. Bearns, Applied Catalysis, 16, 215 (1985)

(6) L.H. Schwartz, J.B. Butt and M. Bearns, Applied Catalysis,

13, 317 (1985)

(7) K.B. Jensen and F.B. Massotch, J. Catal., 92, 98 (1985)

(8) K.B. Jensen and F.B. Massotch, J. Catal., 92, 109 (1985)

(9) G. Lohrengel, M.R. Dass and M. Bearns. " Preparation of Catalysis ". vol II, p41

(10) J. Barrault and C. Renard, Applied catalysis, 14, 133 (1985)

(11) J. Barrault and C. Forquy, Applied Cayalysis, 5, 119 (1983)

(12) W. L. Van Dijk, J.W. Niemantsverdriet, A.M. van der Kraan and H.S. van der Baan, Applied Catalysis, 2, 273 (1982)

(13) R.W. Grant, S. Geller, J.A. Cape, and G.P. Espinosa, Physical Review, 175, 2, 686 (1968)

(14) S. Geller, Acta Cryst. B27, 821 (1971)

(15) Arnulf Muan and Shigeyuki, Amer. J. of Sci, 260, 3, 230 (1962)

(16) E. Banks and E. Kostiner. J of Chem. Phys. 45, 4, 1189 (1966)

(17) E. Banks and E. Kostiner, J. of Appli. Phys. 37, 3, 1423 (1966)

(18) S. Geller, R. L. Grant, J.A. Cape and G. P. Espinosa, J of Appli. Phys. 38, 3, 1457 (1967)

(19) U. Konig, Solid State Commun., 9, 425 (1971)

(20) U. Konig, Phys. Stat. Solidi. 33, 811 (1969)

(21) R. Chandra and S. Lokanathan, Phys. stat. Solidi (b), 83, 273 (1977)

(22) G.A. Sawatzky, J.M.D. Coey and A.H. Morrish, J. of Appli. Phys., 40, 3, 1402 (1969)

(23) F.K. Lotgering, J. Phys. Chem. Solids, 25, 95 (1964)

(24) I. Bunget, Phys. Stat. Solidi, 28, K39 (1968)

(25) M. Boranz, G. Floti, A. Gerberg and M. Rosenberg, J Phys. (C), 2, 1008 (1969)

(26) L. Cser et al, Phys. Stat. Sol. 27, 131 (1968)

(27) E. Wieser, V.A. Poviskii, E.I. Makarov and K. Kleinstuck,

Phys. Stat. Sol. 25, 607 (1968)

(28) F.W. Harrison, W.P. Osmond and R.W. Teale, Phys. Rev., 106, 5, 865 (1957)

(29) V.K. Singh, R. Chandra and S. Lokanathan, Phys. Stat. Sol (B), 105, K13 (1969)

(30) G.A. Sawatzky, F. Van der Wond and A.H. Morrish, Phys. Rev. 187, 2, 747 (1969)

(31) S. Debenedetti, G. Lang and R. Ingalls, Phys. Rev. Letters, 6, 2, 60 (1961)

(32) D.P. Johnson, Solid State Commun. 7, 1785 (1969)

(33) Mossbaure Data index.

(34) D.J. Elias and J.W. Linnet. Trans. Farady Soc., 65, 2673

(35) Nicholas W. Hurst, Stephen J. Gentry and Alan Jones, Catal. Rev. Sci. Eng., 24(2), 233 (1982)

(36) David S. Newsome, Catal. Rev. Sci. Eng., 21(2), 275 (1980)

(37) Satterfield, C.N., and Stenger, H.G., I&EC. Process Des. Dev. 23, 26 (1984)

(38) J.P. Reymond, P. Meriaudeau and S.J. Teichner, J. Catal, 75, 39 (1982)

(39) G.E. Caer, J.M. Dubois, M.Pijolat, V. Perrichon and P. Bussiere, J Phys. Chem. 86, 4799 (1982)

(40) J.A. Amelse, G. Grynkewich, J.B. Butt and L.H. Schwartz, J. Phys. Chem. 85, 2484 (1981)

(41) J.W. Niemantsverdriet, A.M. van der Kraan, W.L. van Dijk and S. van der Baan, J. Phys. Chem. 84, 3363 (1980)

(42) J.A. Amelse, J.B. Butt, and L.H. Schwartz, J.Phys. Chem., 82, 558 (1978)

(43) J.G. Goodwin. Jr and G. Parravano, J. Phys. Chem. 82, 9, 1040 (1978)

(44) G.P. Raupp and W.N. Delgass, J Catal, 58, 348 (1979)

(45) G.J. Huchings and J.C.A. Boeyens, J. Catal. 100, 507 (1986)

(46) Basset, Proceedinfs of the 7th international congress on catalysis, A27

(47) Verma., R.L., Can. J. Chem. Eng. 63, 72 (1985)

(48) M.I. Temkin et al, Kinet. Katal. 6, 1057 (1965)

(49) C.N. Satterfield et al, I.& E.C. Prod. Res. Dev. 25, 407 (1986)

(50) S.J. Tauster and S.C. Fung, J. Catal., 55, 29 (1978)

(51) S.J. Tauster, S.C. Fung, and R.L. Garten, J. Amer. Chem. Soc., 100, 170 (1978)

(52) Dummesic, J.A., J. Catal., 70, 308 (1981)

(53) Dummesic, J.A., J. Catal., 70, 323 (1981)

(54) Dummesic, J.A., J. Catal., 70, 335 (1981)

(55) W.M.H. Sachtler, D.F. Shriver, W.B. Hollenberg and A.F. Lang, J. Catal, 92, 429 (1985)

(56) F.G.A. van der Berg, J.H.E. Glezer, and W.M.H. Sachtler, J. Catal, 93, 340 (1985)

(57) J.W. Niemantsverdriet and A.M. van der Kraan, J. Catal. 72, 385 (1981)

(58) Bennet, C.O., J. Catal., 72, 385 (1981)

(59) Bennet, C.O., J. Catal., 64, 163 (1980)

(60) Bennet, C.O., J. Catal., 89, 327 (1984)

(61) Bennet, C.O., J. Catal., 53, 331 (1978)

Table 1 : Fitted Mössbauer parameters and summarized XRD results of freshly prepared and calcined catalysts

Cat.	pre-treatment	Phase Identified	IS. (mm/s)	QS. (mm/s)	Hf. (koe)	Area[a] Frac.	XRD Pattern and Unit cell Dim.
pure iron	120°C vaccum dried	α-FeOOH	0.39	0.27	335.3	32.2%	hematite
		γ-FeOOH	0.34	0.72	***	67.8%	a=5.03 A (5.035)[b]
							c=13.79A (13.75)
Fe/Mn =9/1	120°C vaccum dried	γ-FeOOH	0.36	0.66	***	100 %	hematite a=4.89 A (5.035) c=13.44A (13.75)
Fe/Mn =1/1	120°C vaccum dried	α-FeOOH	0.34	0.04	393.7	75.1%	γ- Mn_2O_3
		γ-FeOOH	0.34	0.72	***	24.9%	a=5.82 A (5.73)
							c=9.49 A (9.33)
Fe/Mn =1/9	120°C vaccum dried	α-FeOOH	0.31	0.27	395.9	63.8%	γ- Mn_2O_3
		γ-FeOOH	0.33	0.85	***	36.2%	a=5.76 A (5.73)
							c=9.45 A (9.33)
pure Mn	120°C vaccum dried	***	**	**	***	***	γ- Mn_2O_3 a=5.74 A (5.73) c=9.37 A (9.33)
pure iron	500°C cal-cined	α-Fe_2O_3	0.36	0.23	512.5	70.6%	hematite
		Fe^{+3}	0.33	0.26	***	29.4%	a=5.04 A (5.03)
							c=13.77A (13.79)
Fe/Mn =9/1	500°C cal-cined	α-$(Fe_{1-x}Mn_x)_2O_3$	0.37	0.23	505.6	100%	hematite a=4.97 A (5.03) c=13.69A (13.79)
Fe/Mn =1/1	500°C cal-cined	α-$(Fe_{1-x}Mn_x)_2O_3$	0.37	0.20	502.1	60.5%	hematite c=13.75A (13.79) a=5.03 A (5.03)
		β-$(Mn_{1-y}Fe_y)_2O_3$					cubic Mn_2O_3
		8(a)site	0.38	1.10	***	25.0%	a=9.415A (9.41)
		24(d)site	0.37	0.72	***	14.6%	
Fe/Mn =1/9	500°C cal-cined	β-$(Mn_{1-y}Fe_y)_2O_3$					
		8(a)site	0.39	1.17	***	51.3%	cubic Mn_2O_3
		24(d)site	0.37	0.66	***	48.7%	a=9.42 A (9.41)
pure Mn	500°C cal-cined	***	**	**	***		cubic Mn_2O_3 a=9.41 A (9.41)

a: It is iron content if it is assumed recoiless fractions are the same
b: A.S.T.M standard value for unit cell distance

Table 2 : Fitted Mössbauer parameter and summarized XRD results of high and low temperature reduced catalysts

Cat.	Pre-treatment	Phase Identified	IS. (mm/s)	QS. (mm/s)	Hf (koe)	FWHM [c] (mm/s)	Area [a] frac.	XRD Pattern Unit cell dimensions
pure iron	500°C H_2 redn.	α-iron	.0065	.0063	341.8	0.37	100%	α-iron
Fe/Mn =9/1	500°C H_2 redn.	α-iron	.0058	.0026	339.1	0.31	88.9%	α-iron
		$Mn_{3-y}Fe_yO_4$	0.36	0.84	***	0.59	6.3%	Mn_3O_4 a=8.78A (8.7) [b]
		$Fe_{1-z}Mn_zO$	1.07	0.69	***	0.33	4.8%	MnO a=4.36A (4.445)
Fe/Mn =1/1	500°C H_2 redn.	α-iron	.0045	.0025	325.0	0.39	80.8%	α-iron
		$Mn_{3-y}Fe_yO_4$	0.43	1.21	***	0.87	9.0%	Mn_3O_4 a=8.64A (8.7)
		$Fe_{1-z}Mn_zO$	0.93	0.54	***	0.53	10.2	MnO a=4.41A (4.445)
Fe/Mn =1/9	500°C H_2 redn.	α-iron	.0034	.0014	327.9	0.36	75.5%	α-iron
		$Mn_{3-y}Fe_yO_4$	0.27	0.67	***	0.42	6.0%	Mn_3O_4
		$Fe_{1-z}Mn_zO$	0.90	0.22	***	0.37	18.5%	MnO a=4.42A (4.445)
pure iron	330°C H_2 redn.	α-iron	.0058	.0046	337.9	0.33	85.7%	α-iron
		Fe_3O_4(a)	0.28	0.20	500.8	0.24	3.7%	megnatite
		Fe_3O_4(b)	0.66	0.02	468.6	0.47	10.6%	
Fe/Mn =9/1	330°C H_2 redn.	α-iron	.0044	0.04	330.4	0.56	14.2%	α-iron
		$Fe_{3-x}Mn_xO_4$(a)	0.25	0.05	486.4	0.42	5.8%	megnatite
		(b)	0.50	0.04	447.9	1.17	13.3%	
		$Mn_{3-y}Fe_yO_4$	0.36	.004	***	2.58	25.6%	Mn_3O_4
		$Fe_{1-z}Mn_zO$	1.05	0.59	***	0.59	41.2%	MnO
Fe/Mn =1/1	330°C H_2 redn.	$Mn_{3-y}Fe_yO_4$	0.18	0.50	***	0.62	51.8%	Mn_3O_4 a=8.64A (8.7)
		$Fe_{1-z}Mn_zO$	1.12	0.62	***	0.54	48.2%	MnO a=4.36A(4.445)
Fe/Mn =1/9	330°C H_2 redn.	$Mn_{3-y}Fe_yO_4$	0.33	0.62	***	0.56	57.0%	Mn_3O_4 a=8.68A (8.7)
		$Fe_{1-z}Mn_zO$	1.08	0.57	***	0.56	43.0%	MnO a=4.43A(4.445)

a: It's relative iron conc. if recoiless fractions are the same
b: A.S.T.M. standard value of unit cell dimension.
c: F.W.H.M represents width of peaks at half height, for sextet, it is the width of the outest line.

Table 3 : Mössbaure parameters of 1/1, 1/9 catalysts reduced at 330° C in hydrogen for 12 hrs taken at an expanded velocity scale

Catalyst	Phase identified	IS. (mm/s)	QS. (mm/s)	FWHM[c] (mm/s)	Area[a] Fraction
Fe/Mn=1/1	$Fe_{1-z}Mn_zO$ (I)	0.804	1.066	0.576	22.62%
	$Fe_{1-z}Mn_zO$ (II)	0.997	0.940	0.599	33.25%
	$Mn_{3-y}Fe_yO_4$ (I)	0.378	0.593	0.264	8.31%
	$Mn_{3-y}Fe_yO_4$ (II)	0.356	0.952	0.599	35.82%
Fe/Mn=1/9	$Fe_{1-z}Mn_zO$ (I)	1.028	0.598	0.541	30.56%
	$Fe_{1-z}Mn_zO$ (II)	1.160	0.614	0.521	24.71%
	$Mn_{3-y}Fe_yO_4$ (I)	0.320	0.550	0.540	33.42%
	$Mn_{3-y}Fe_yO_4$ (II)	0.328	1.018	0.431	11.30%

a: It's relative iron conc. if recoiless fractions are the same
c: F.W.H.M represents width of peaks at half height, for sextet, it is the width of the outest line.

Table 4 : Mössbauer parameters of high and low temperature reduced, used catalysts

Cat.	Pre-treatment	Phase Identified	IS. (mm/s)	QS. (mm/s)	Hf (koe)	FWHM.[c] (mm/s)	Area[a] frac.	XRD Pattern Unit cell dimensions
pure iron	500°C H_2 redn. 320°C rexn.	Fe_3O_4(a)	0.310	0.46	500.8	0.43	5.7%	magnetite
		Fe_3O_4(b)	0.677	0.09	467.4	0.48	10.2%	
		χ-Fe_5C_2(I)	0.275	0.00	221.2	0.43	33.4%	χ-carbide
		χ-Fe_5C_2(II)	0.203	0.00	189.4	0.48	30.3%	
		χ-Fe_5C_2(III)	0.217	0.00	109.9	0.44	17.8%	
		Fe^{+3}	0.195	1.07	***	0.25	2.6%	
Fe/Mn =9/1	500°C H_2 redn. 320C rexn.	$Fe_{3-x}Mn_xO_4$(a)	0.323	0.05	497.5	0.33	3.7%	magnetite
		$Fe_{3-x}Mn_xO_4$(b)	0.669	0.15	462.1	0.74	7.6%	
		α-iron	0.007	.017	337.7	0.32	21.0%	α-iron
		χ-Fe_5C_2(I)	0.242	0.00	215.5	0.44	27.5%	χ-carbide
		χ-Fe_5C_2(II)	0.155	0.00	193.7	0.45	21.3%	
		χ-Fe_5C_2(III)	0.286	0.00	110.9	0.25	5.8%	
		$Mn_{3-y}Fe_yO_4$	0.451	0.99	***	0.77	7.5%	
		$Fe_{1-z}Mn_zO$	1.101	0.94	***	0.56	5.5%	
Fe/Mn =1/1	500°C H_2 redn. 320C rexn.	$Fe_{3-x}Mn_xO_4$(a)	0.290	0.04	483.4	0.34	3.4%	magnetite
		$Fe_{3-x}Mn_xO_4$(b)	0.534	0.18	446.8	0.94	10.0%	
		ε-$Fe_{2.2}C$	0.235	0.11	180.9	0.57	9.5%	
		$Mn_{3-y}Fe_yO_4$	0.174	0.48	***	0.58	27.4%	Mn_3O_4 a=8.72A(8.7)[b]
		$Fe_{1-z}Fe_zO$	1.082	0.61	***	0.51	49.7%	MnO a=4.41A(4.445)
Fe/Mn =1/9	550°C H_2 redn. 320C rexn.	χ-Fe_5C_2(I)	0.251	0.10	212.3	0.38	21.8%	χ-carbide
		χ-Fe_5C_2(II)	0.170	0.08	186.9	0.45	21.8%	
		χ-Fe_5C_2(III)	0.298	0.01	107.5	0.44	10.9%	
		$Fe_{1-z}Mn_zO$	1.066	0.27	***	0.41	16.7%	MnO a=4.38A(4.445)
		$Mn_{3-y}Fe_yO_4$	0.374	0.89	***	0.52	28.7%	Mn_3O_4
pure iron	330°C H_2 redn. 320°C rexn.	Fe_3O_4(a)	0.273	0.32	488.9	0.42	17.8%	magnetite
		Fe_3O_4(b)	0.656	0.026	458.9	0.44	27.5%	
		χ-Fe_5C_2(I)	0.280	0.00	215.1	0.41	21.6%	χ-carbide
		χ-Fe_5C_2(II)	0.216	0.00	188.2	0.44	19.8%	
		χ-Fe_5C_2(III)	0.156	0.00	116.3	0.40	11.1%	
		Fe^{+3}	0.157	1.02	***	0.27	2.2%	
Fe/Mn =9/1	330°C H_2 redn. 320°C rexn.	$Fe_{3-x}Mn_xO_4$(a)	0.270	0.03	484.7	0.37	20.5%	magnetite
		$Fe_{3-x}Mn_xO_4$(b)	0.644	0.05	455.3	0.62	39.2%	
		χ-Fe_5C_2(I)	0.250	0.11	214.3	0.45	12.6%	χ-carbide
		χ-Fe_5C_2(II)	0.228	0.08	184.2	0.47	12.7%	
		χ-Fe_5C_2(III)	0.213	0.00	103.6	0.39	6.3%	
		$Fe_{1-z}Mn_zO$	0.879	0.87	***	0.45	2.5%	MnO
		$Mn_{3-y}Fe_yO_4$	0.342	0.75	***	0.45	6.1%	Mn_3O_4

to be continued

Fe/Mn =1/9	330C H_2 redn. 320C rexn.	$Mn_{3-y}Fe_yO_4$	0.361	0.77	***	0.59	84.0%	Mn_3O_4
		$Fe_{1-z}Mn_zO$	1.112	0.73	***	0.54	16.4%	MnO

a: It's relative iron conc. if recoiless fractions are the same
b: A.S.T.M. standard value of unit cell dimension.
c: F.W.H.M represents width of peaks at half height, for sextet, it is the width of the outest line.

Table 5 : Mössbauer parameters of 1/1, 1/9 catalysts reduced at 330 °C in hydrogen for 12 hrs taken at an expanded velocity scale

Catalyst	Phase identified	IS. (mm/s)	QS. (mm/s)	FWHM. (mm/s)	Area Fraction
Fe/Mn=1/1	$Fe_{1-z}Mn_zO$ (I)	0.804	1.066	0.576	22.62%
	$Fe_{1-z}Mn_zO$ (II)	0.997	0.940	0.599	33.25%
	$Mn_{3-y}Fe_yO_4$ (I)	0.378	0.593	0.264	8.31%
	$Mn_{3-y}Fe_yO_4$ (II)	0.356	0.952	0.599	35.82%
Fe/Mn=1/9	$Fe_{1-z}Mn_zO$ (I)	1.028	0.598	0.541	30.56%
	$Fe_{1-z}Mn_zO$ (II)	1.160	0.614	0.521	24.71%
	$Mn_{3-y}Fe_yO_4$ (I)	0.320	0.550	0.540	33.42%
	$Mn_{3-y}Fe_yO_4$ (II)	0.328	1.018	0.431	11.30%

Table 6 : Mössbaure parameters of 330 °C and 270 °C carbonoxide pretreated catalysts after synthesis

Cat.	Pre treat ment	Phase Identified	IS. (mm/s)	QS. (mm/s)	Hf (koe)	FWHM (mm/s)	Area frac.	XRD Pattern Unit cell dimensions
Fe/Mn =9/1	330C CO H2 320C rexn	Fe3-xMnxO4(t)	0.283	0.031	486.6	1.01	41.3%	magnetite
		Fe3-xMnxO4(o)	0.637	0.052	454.9	0.75	54.3%	
		Fe1-zMnzO	1.111	0.866	***	0.41	4.4%	MnO
Fe/Mn =1/1	330C CO H2 320C rexn	Fa3-xMnxO4(t)	0.297	0.000	481.6	0.54	10.7%	magnetite
		Fe3-xMnxO4(o)	0.528	0.128	445.8	0.91	16.8%	
		X-Fe2.5C(I)	0.174	0.000	208.1	0.49	21.0%	X-Fe2.5C
		X-Fe2.5C(II)	0.241	0.000	171.5	0.43	22.5%	
		X-Fe2.5C(III)	0.179	0.000	111.9	0.12	1.4%	
		Mn3-yFeyO4	0.305	0.844	***	0.78	18.5%	Mn3O4
		Fe1-zFezO4	1.008	0.576	***	0.64	9.0%	MnO
Fe/Mn =1/9	330C CO H2 320C rexn	ϵ'-Fe2.2C	0.203	0.119	172.0	0.36	11.1%	
		Fe1-zMnzO	1.064	0.527	***	0.47	22.4%	MnO
		Mn3-yFeyO4	0.367	0.872	***	0.63	66.5%	Mn3O4
Fe/Mn =1/1	270C CO H2 320C rexn	Fe3-xMnxO4(t)	0.285	0.021	485.7	0.43	22.3%	magnetite
		Fe3-xMnxO4(o)	0.560	0.069	453.2	0.91	46.9%	
		-Fe2.2C	0.231	0.100	171.0	0.56	15.4%	
		Fe1-zMnzO	1.477	1.130	***	0.50	4.9%	MnO
		Mn3-yFeyO4	0.202	0.648	***	0.67	10.5%	Mn3O4
Fe/Mn =1/9	270C CO	ϵ'-Fe2.2C	0.101	0.000	177.1	0.62	9.5%	
		Fe1-zMnzO	1.112	0.734	***	0.54	14.5%	MnO
		Mn3-yFeyO4	0.361	0.734	***	0.59	76.0%	Mn3O4

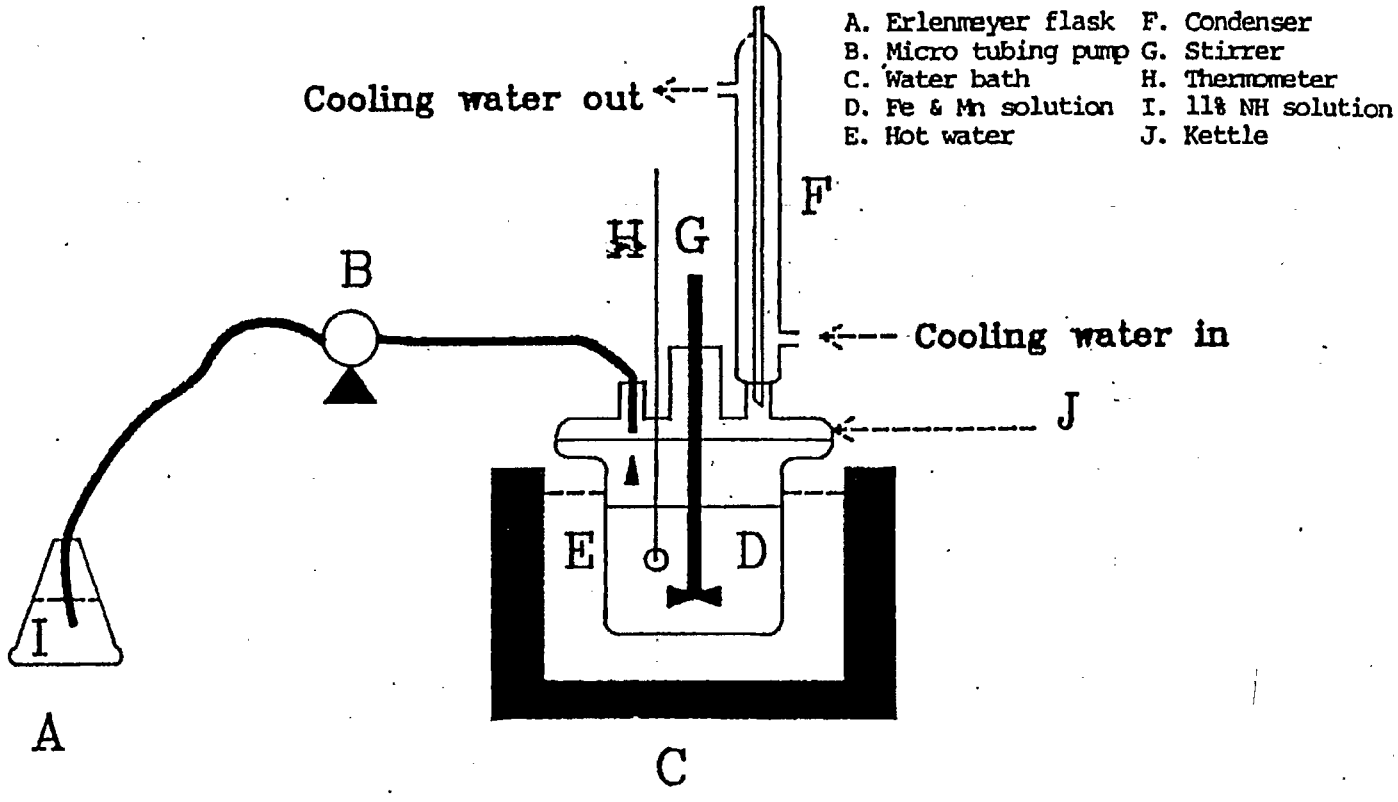

Fig. 1 Apparatus for catalyst preparation.

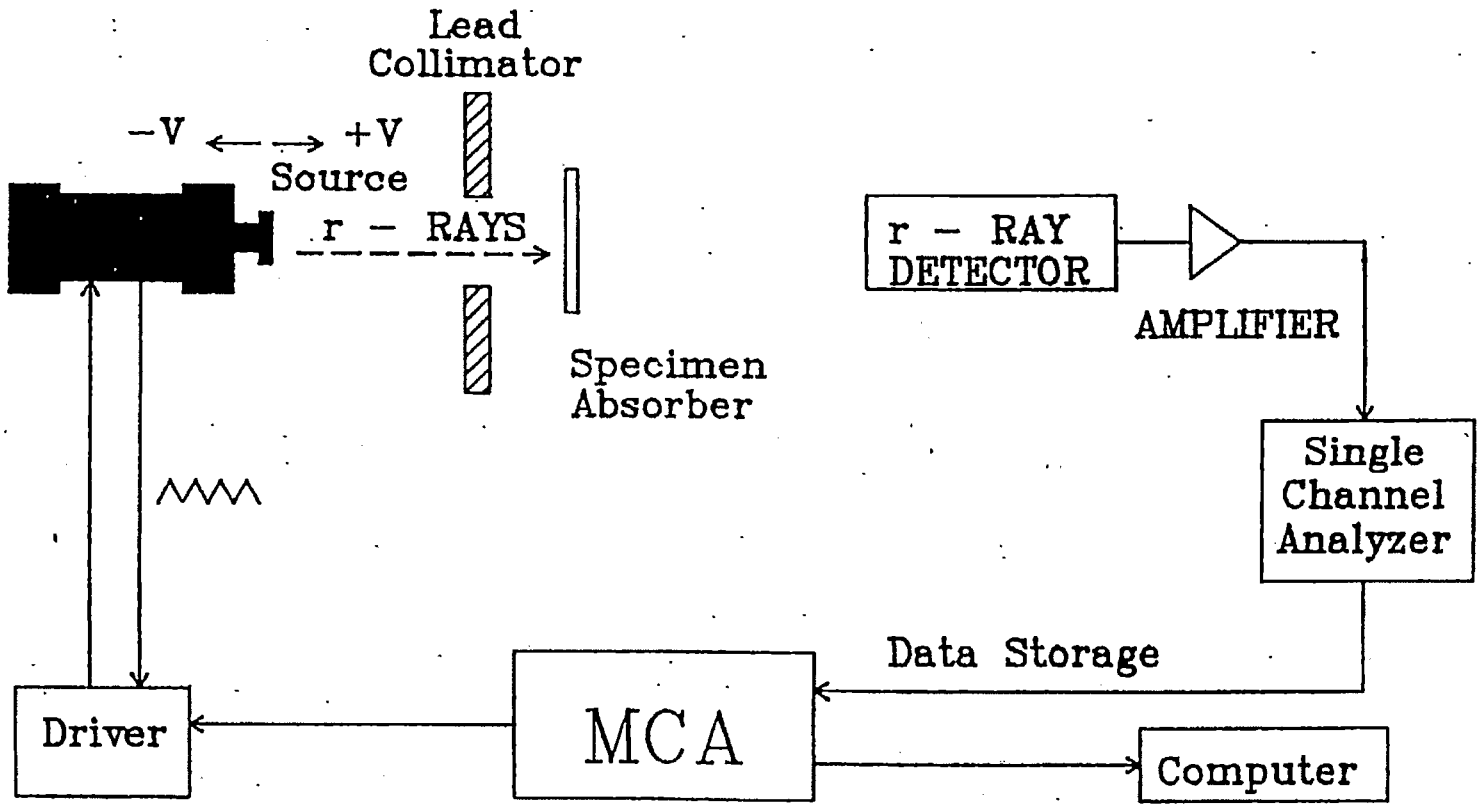

Fig. 2 Schematic diagrm of Mossbauer spectroscopy.

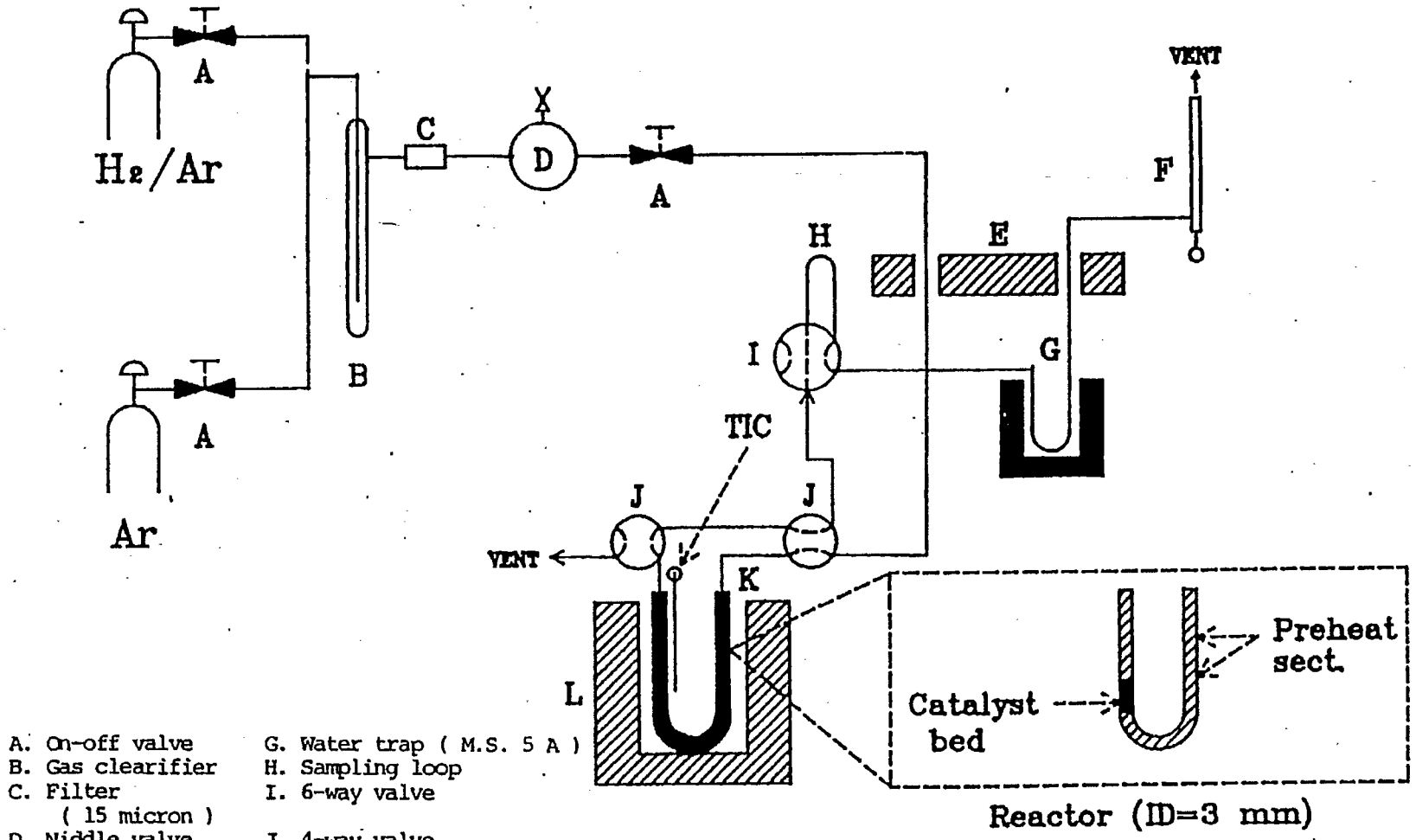

A. On-off valve
B. Gas clearifier
C. Filter (15 micron)
D. Niddle valve
E. G.C.
F. Bubble flowmeter
G. Water trap (M.S. 5 A)
H. Sampling loop
I. 6-way valve
J. 4-way valve
K. Reactor
L. Furnace
TIC. Temperature indicator & controller

Fig. 3 Experimental set-up of TPR system.

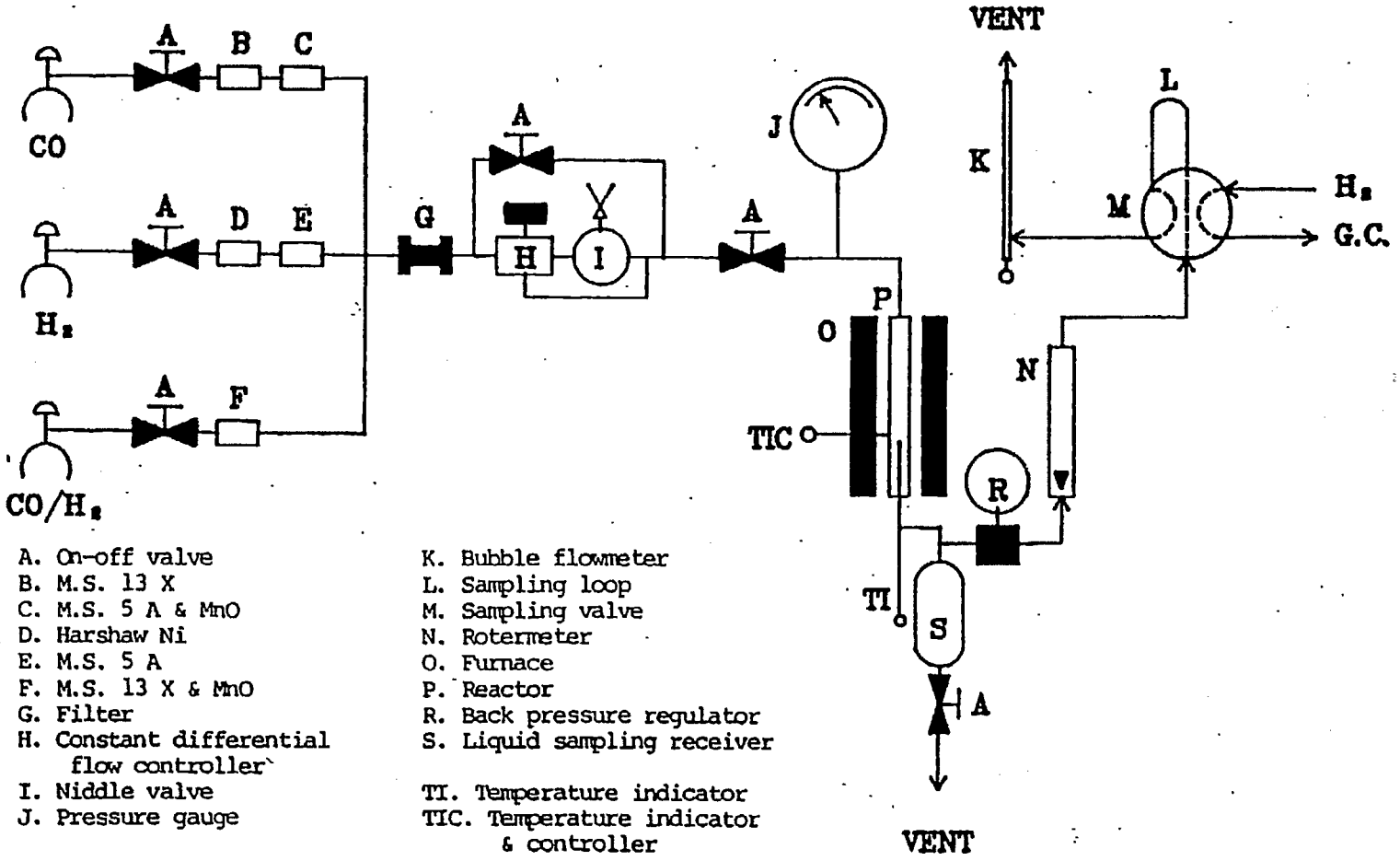

A. On-off valve
B. M.S. 13 X
C. M.S. 5 A & MnO
D. Harshaw Ni
E. M.S. 5 A
F. M.S. 13 X & MnO
G. Filter
H. Constant differential flow controller
I. Niddle valve
J. Pressure gauge

K. Bubble flowmeter
L. Sampling loop
M. Sampling valve
N. Rotermeter
O. Furnace
P. Reactor
R. Back pressure regulator
S. Liquid sampling receiver

TI. Temperature indicator
TIC. Temperature indicator & controller

Fig. 4 Experimental set-up of reaction system.

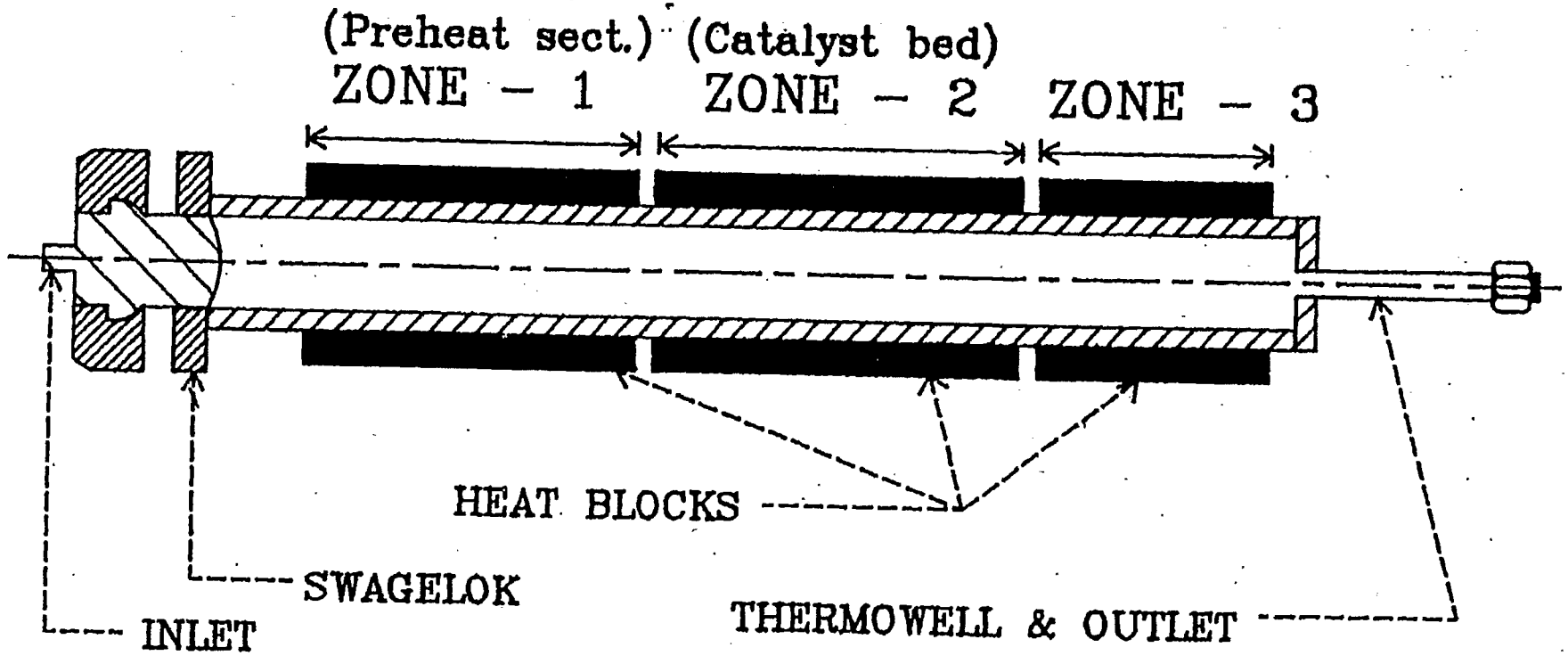

Fig. 5 Cross section of reactor.

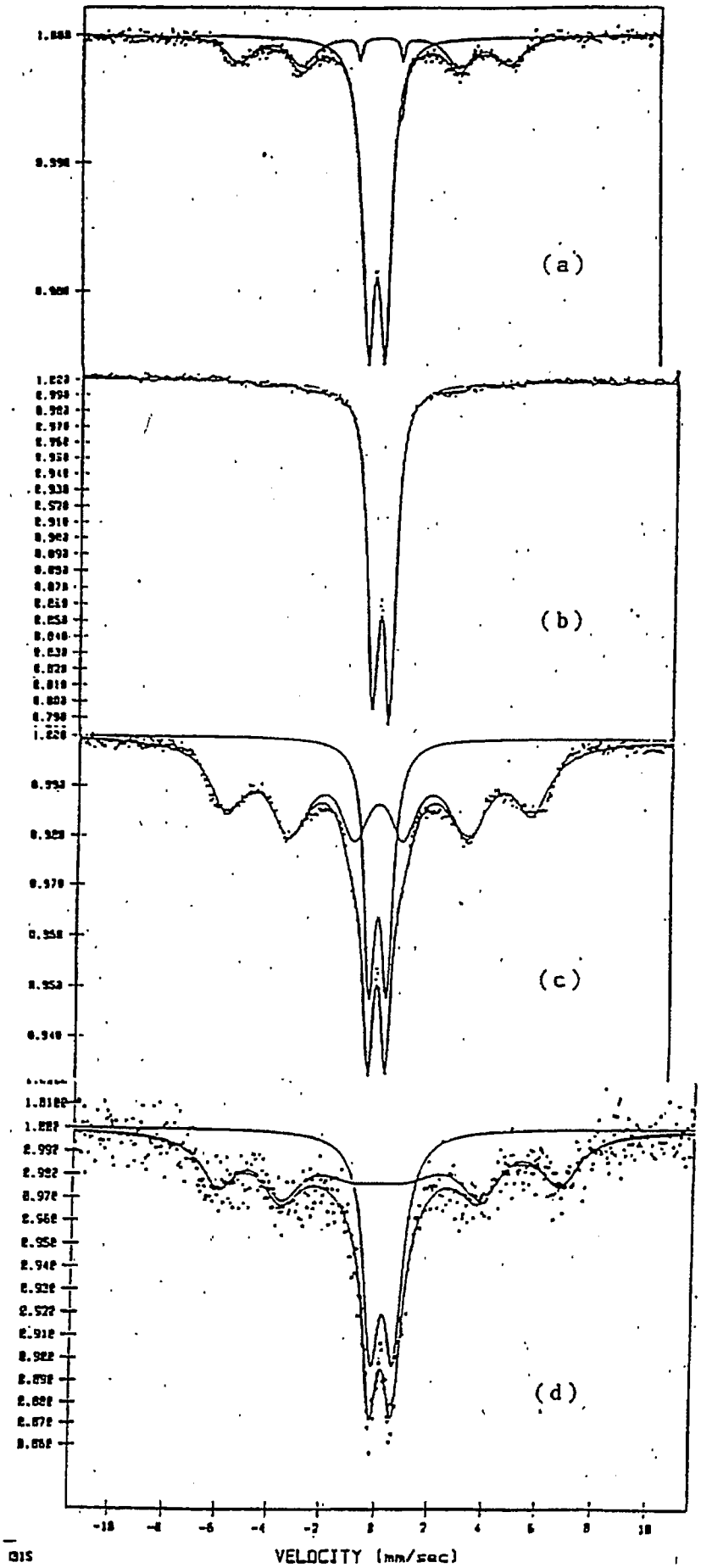

Fig. 6 Mossbauer spectra of uncalcined catalysts.
(a) pure iron, (b) Fe/Mn = 1/1, (c) Fe/Mn = 9/1, (d) Fe/Mn = 1/9

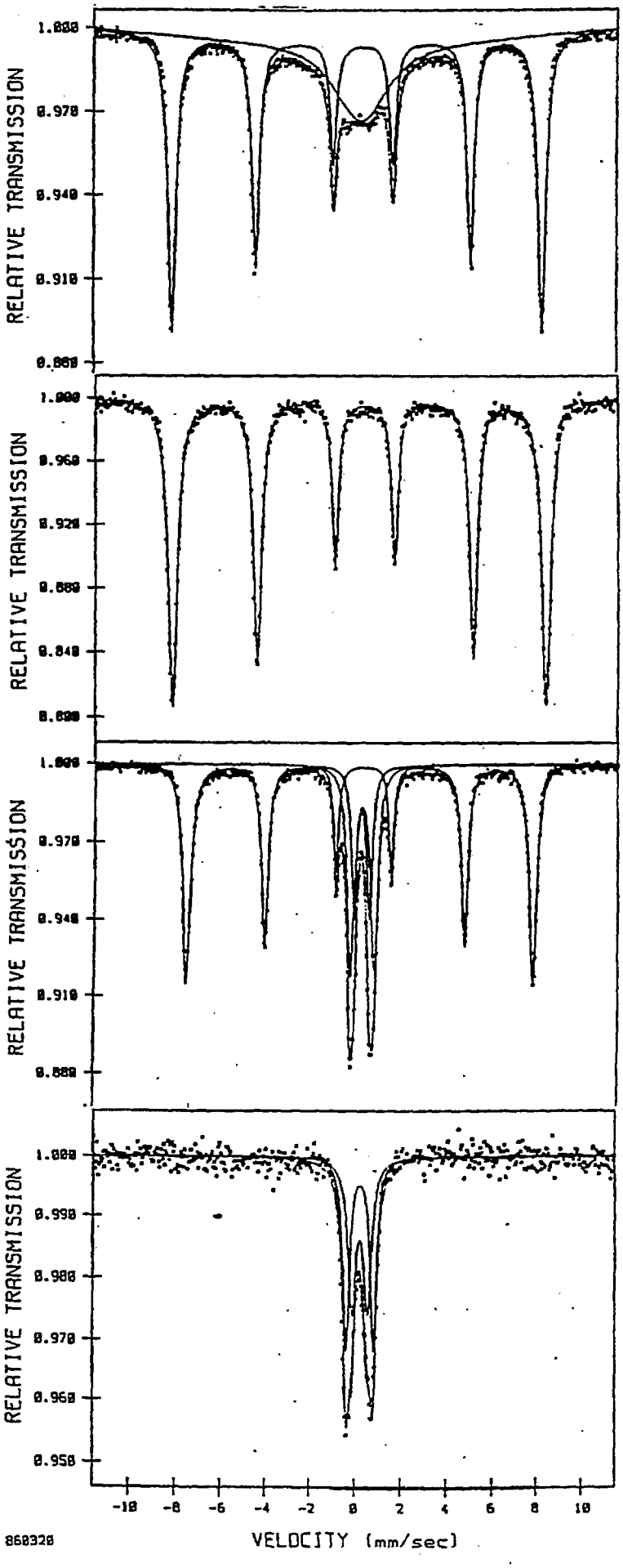

Fig. 7 Mossbauer spectra of catalysts cacined at 500 C in argon.

(a) pure iron, (b) Fe/Mn = 9/1, (c) Fe/Mn = 1/1, (d) Fe/Mn = 1/9

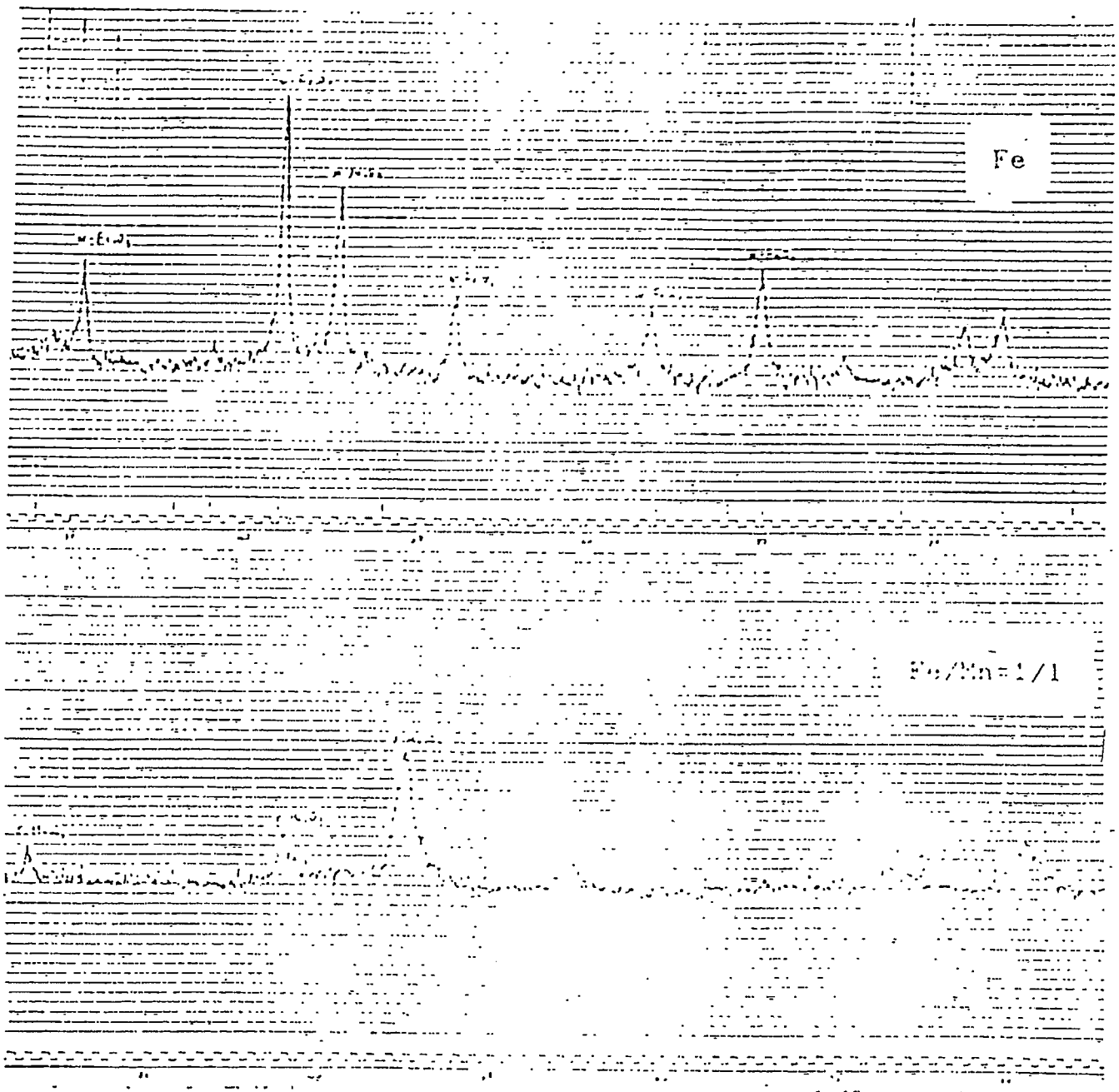

Fig. 8 (a) XRD spectra of unpromoted catalysts

Fig. 81

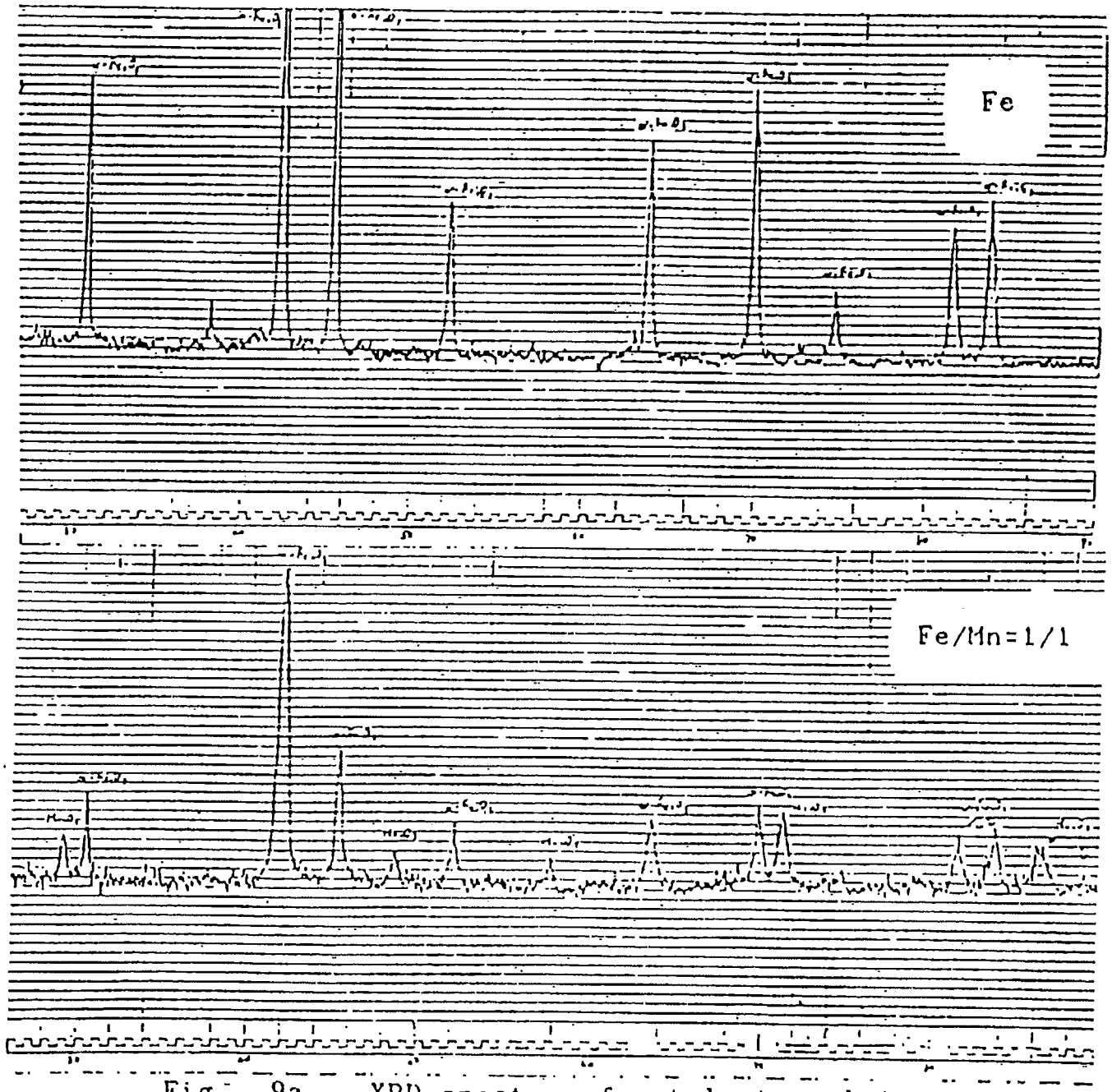

Fig. 9a XRD spectra of catalysts calcined at 500 °C for 5 hr

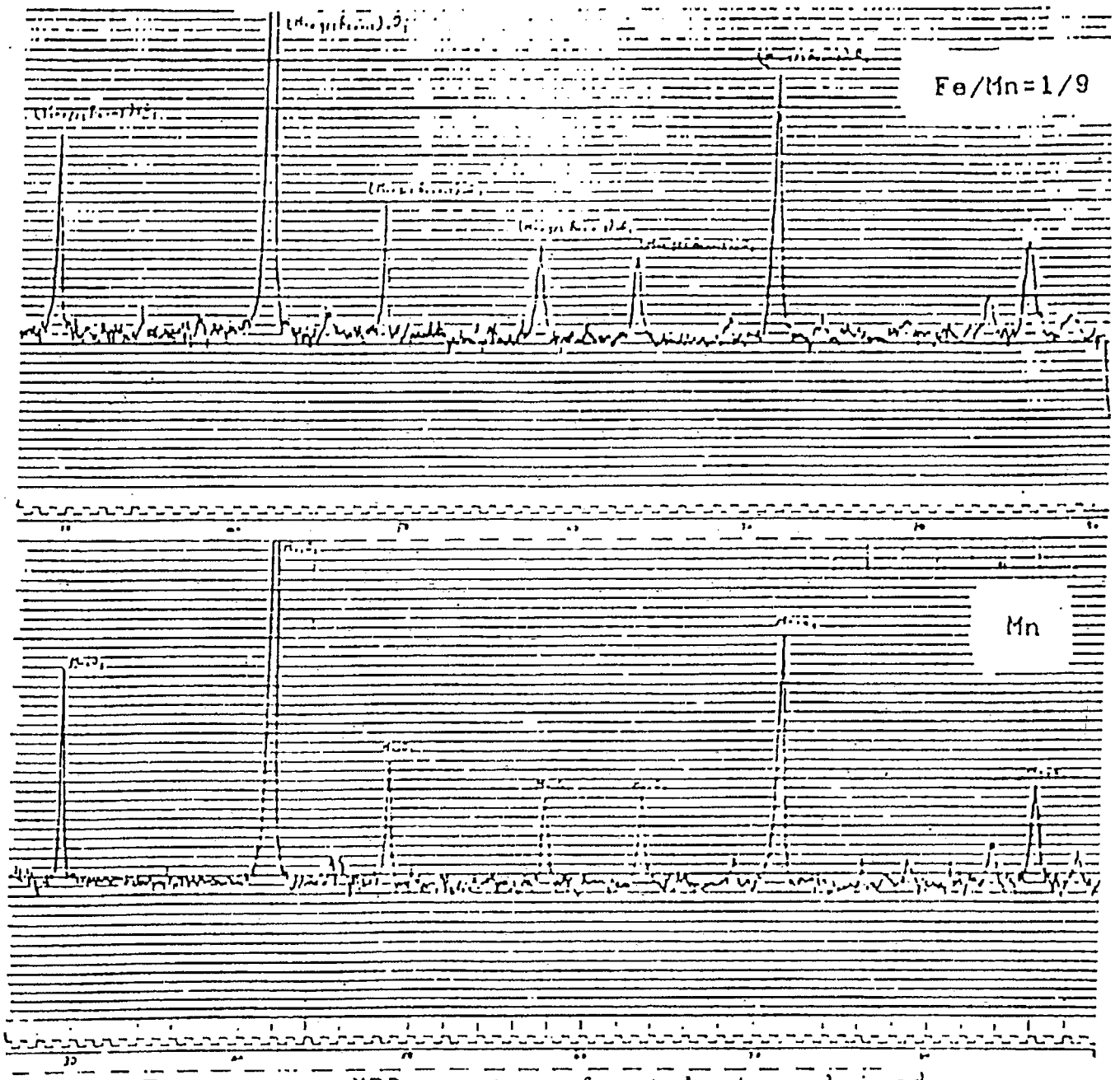

Fig. 9b XRD spectra of catalysts calcined at 500 °C for 5 hr

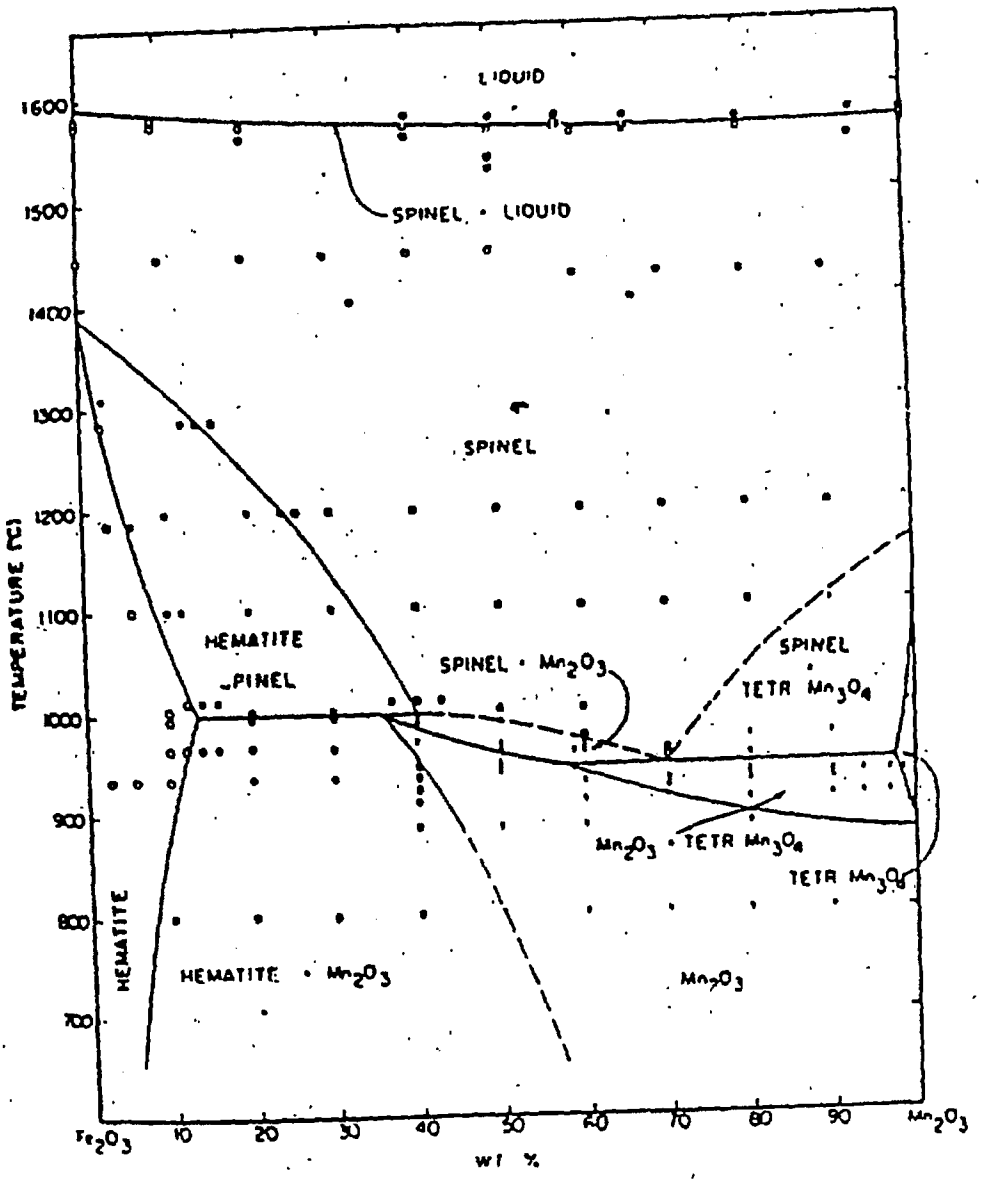

Fig. 10 Phase diagram of (Fe,Mn)O system (15).

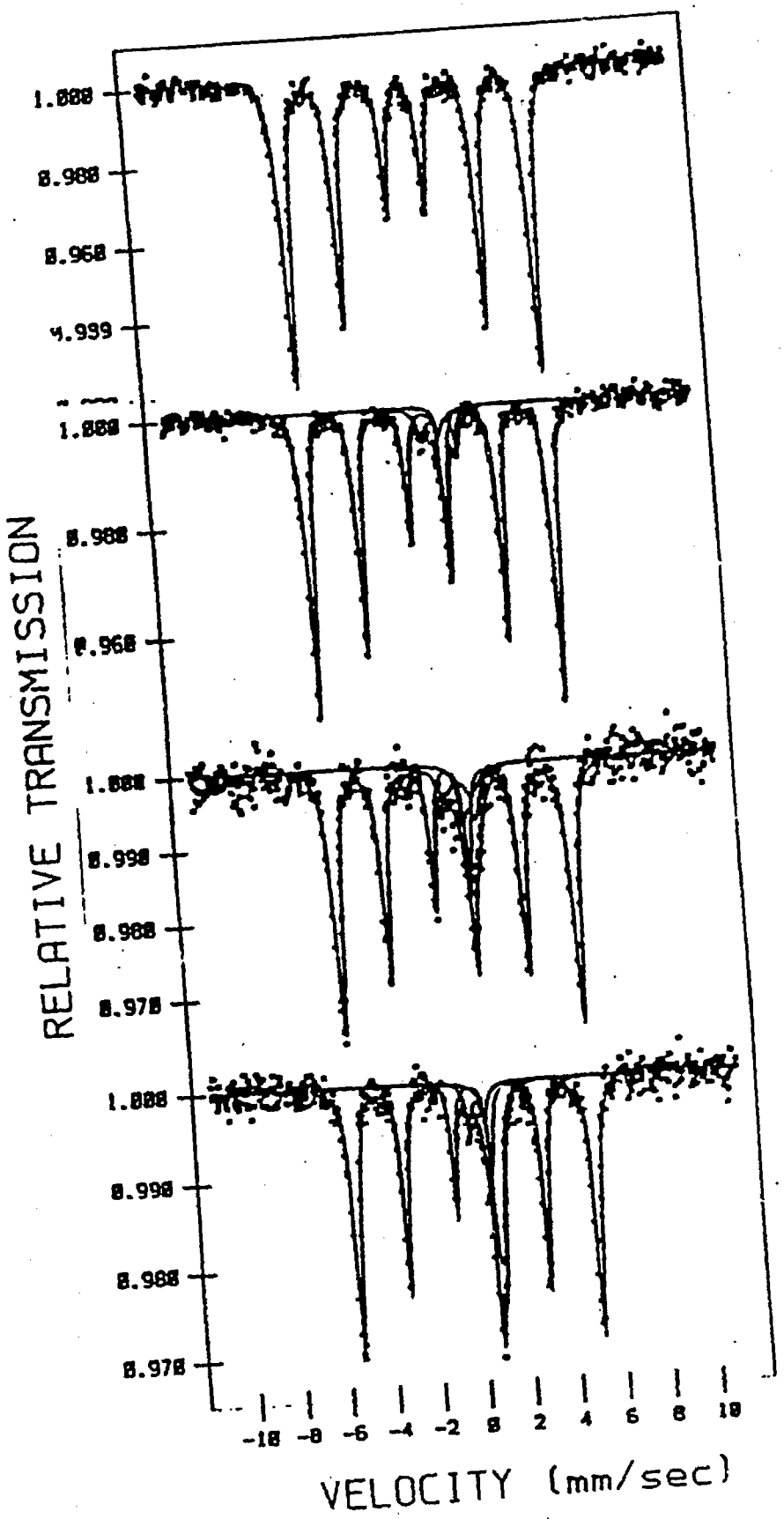

Fig. 11 Mössbauer spectra of Fe-Mn catalysts reduced in hydrogen at 500°C, from top to bottom, pure iron, Fe/Mn=9/1, Fe/Mn=1/1, Fe/Mn=1/9

Fig. 12 XRD spectrum of catalyst Fe-Mn-1 reduced at 500 C in H_2 for 2 h.

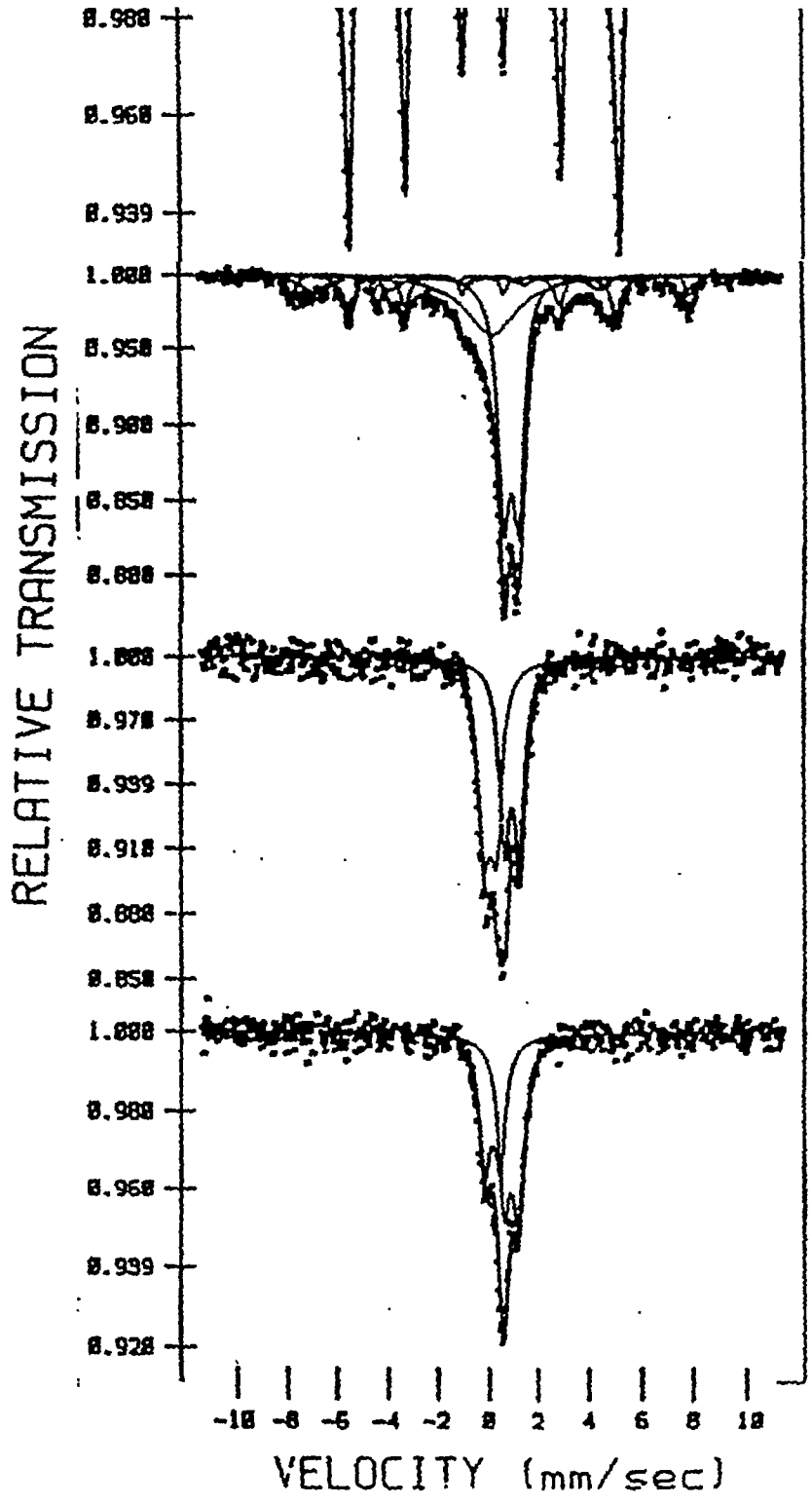

Fig. 13 Mossbauer spectra of Fe-Mn catalysts red
hydrogen at 330°C, from top to bottom, pu
iron, Fe/Mn=9/1, Fe/Mn=1/1, Fe/Mn=1/9.

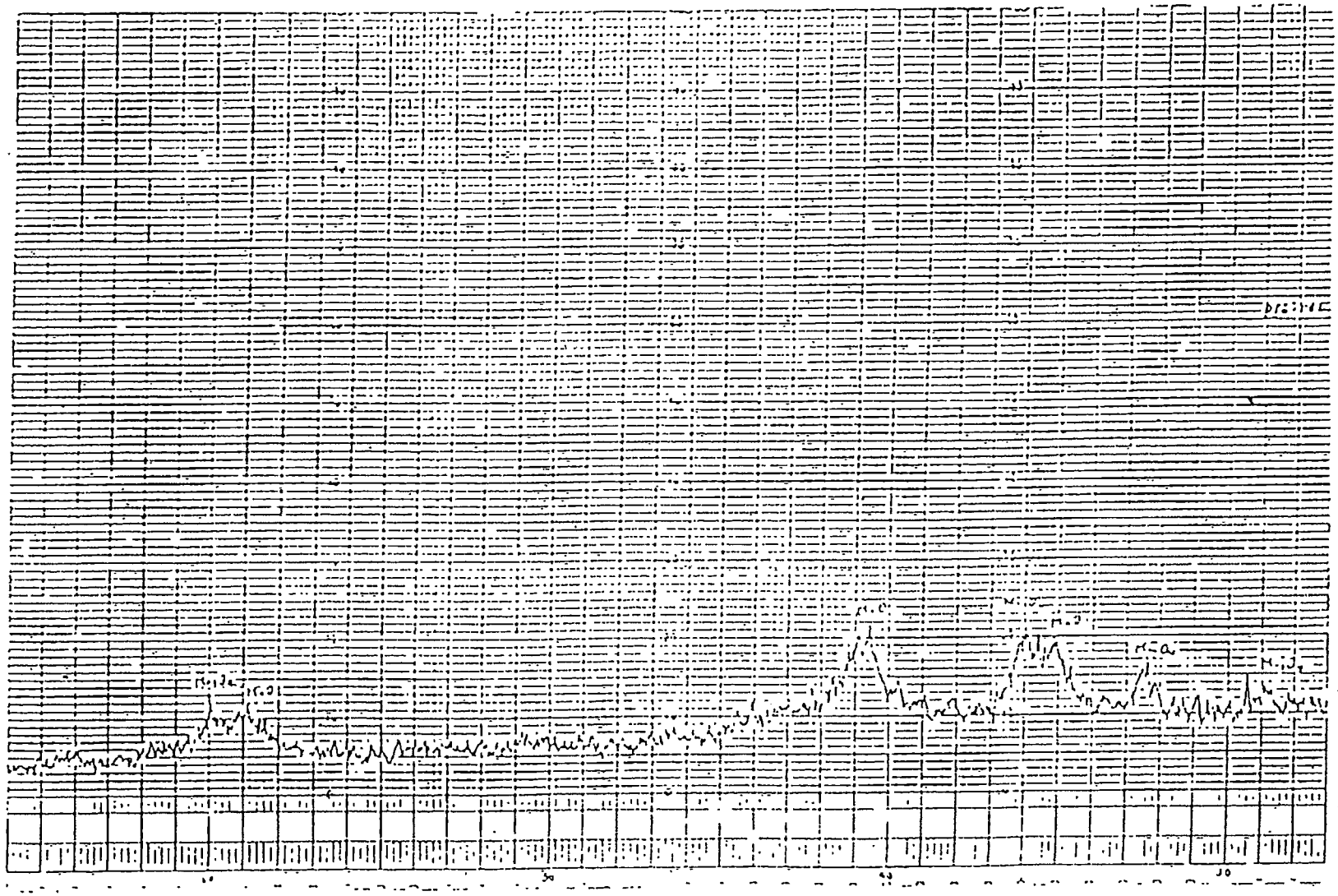

Fig. 14 XRD spectrum of catalyst Fe/Mn=1/9 reduced at 330 C in hydrogen.

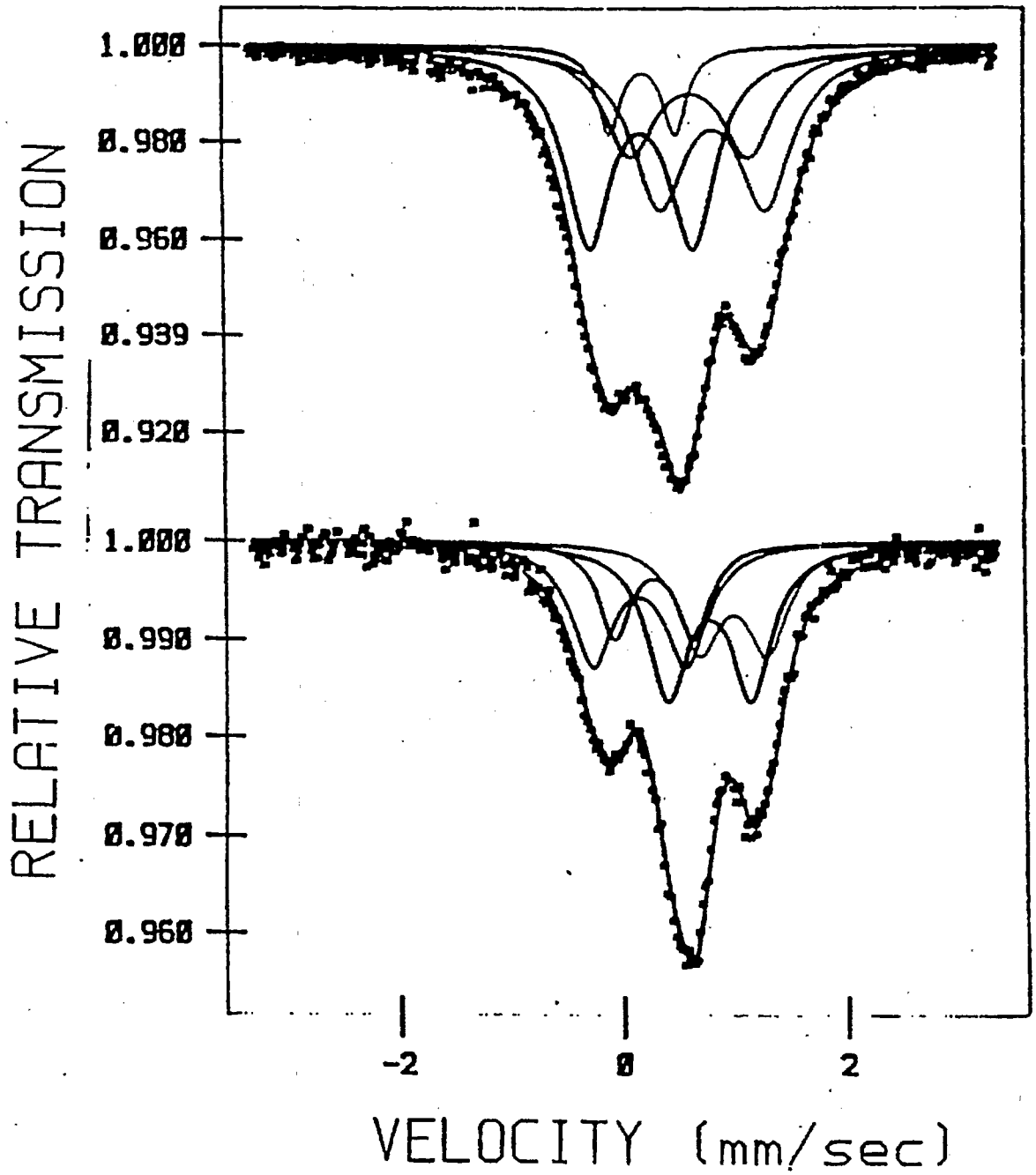

Figure 15: Mössbauer spectra of Fe/Mn=1/1, Fe/Mn=1/9 catalysts taken on an expended velocity scale, top: Fe/Mn=1/1, bottom: Fe/Mn=1/9.

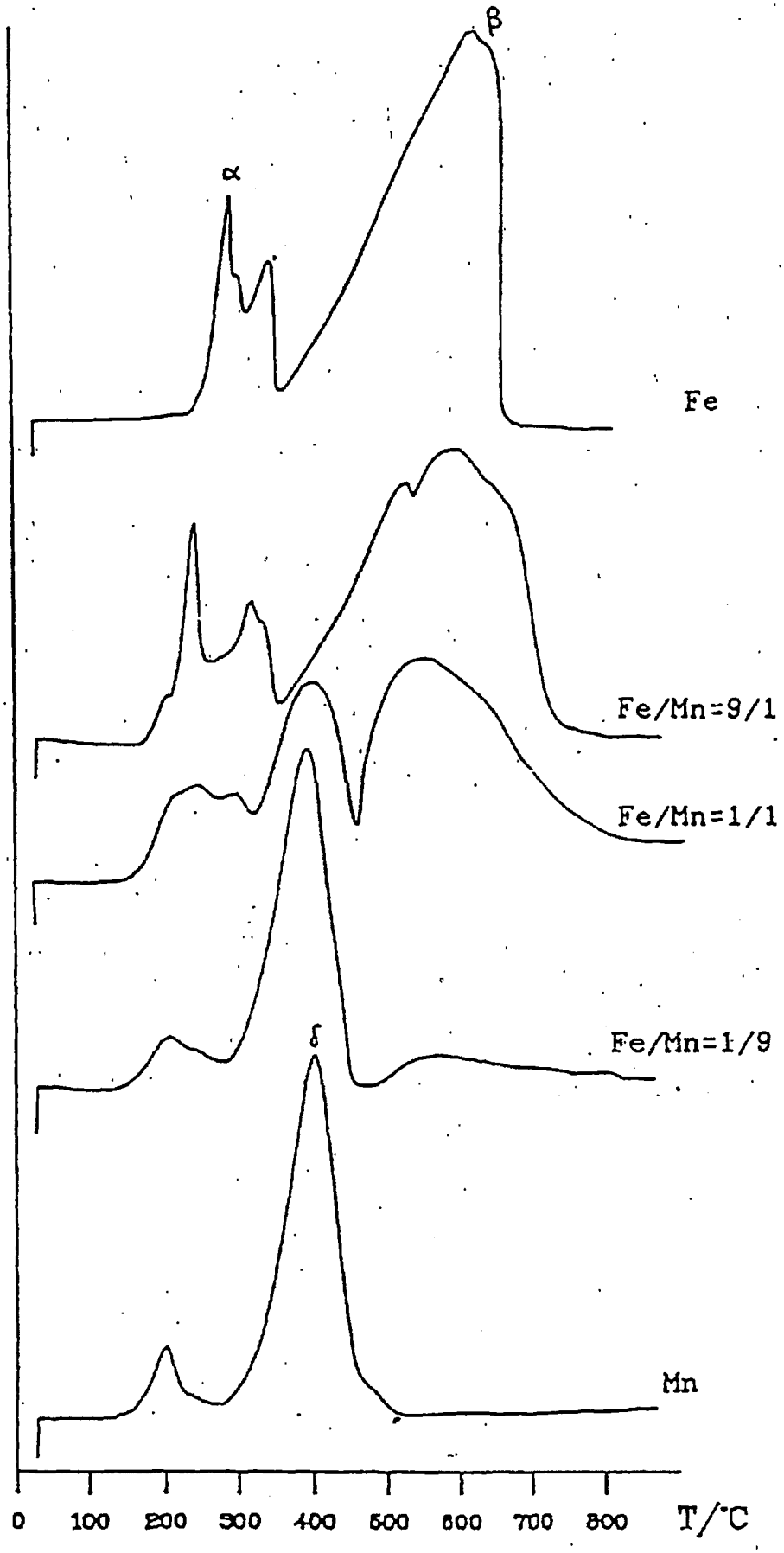

Fig. 16 TPR of uncalcined catalysts

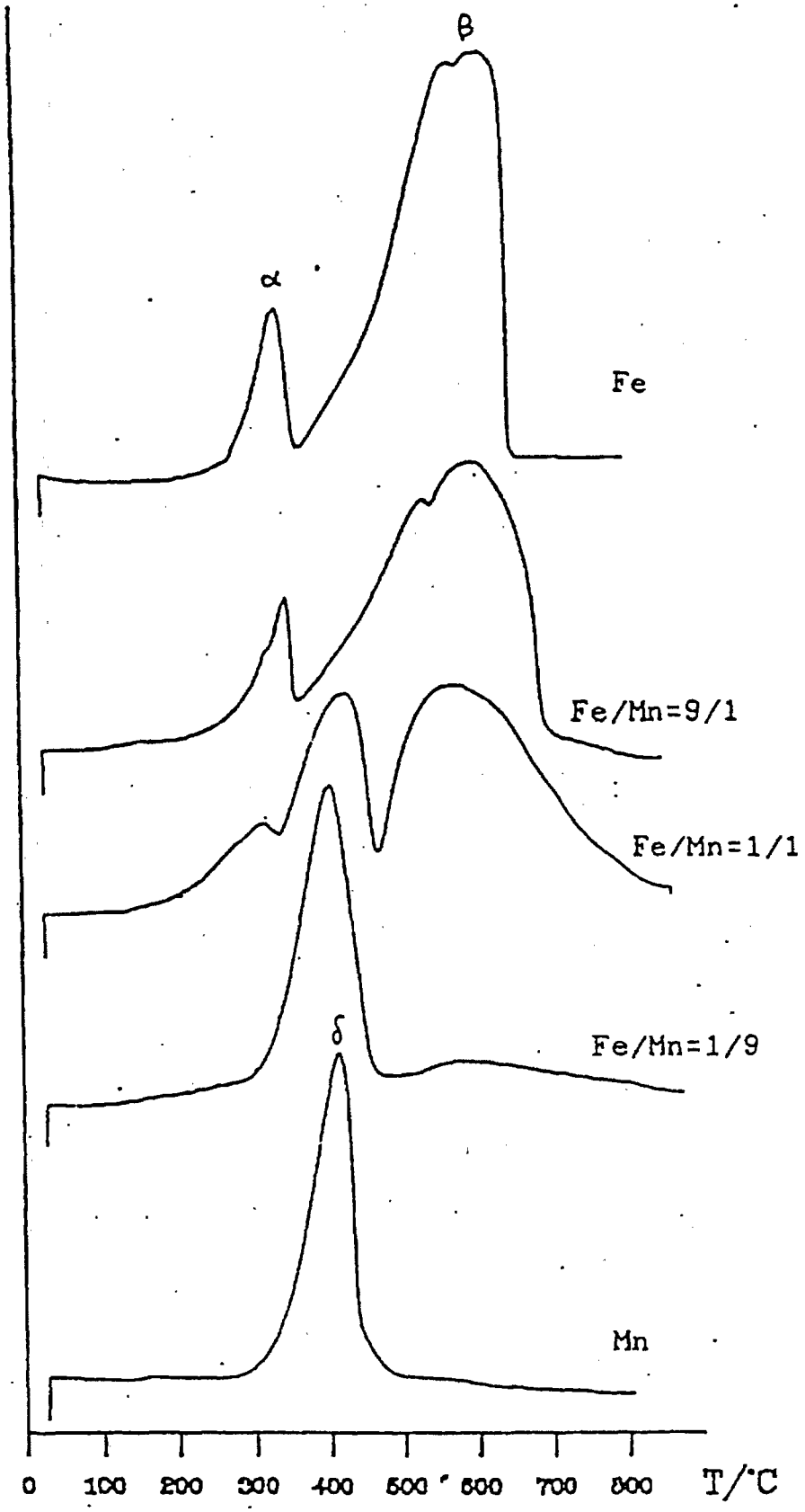

Fig. 17 TPR of catalysts
(calcined at 502 °C in Ar for 5 hr)

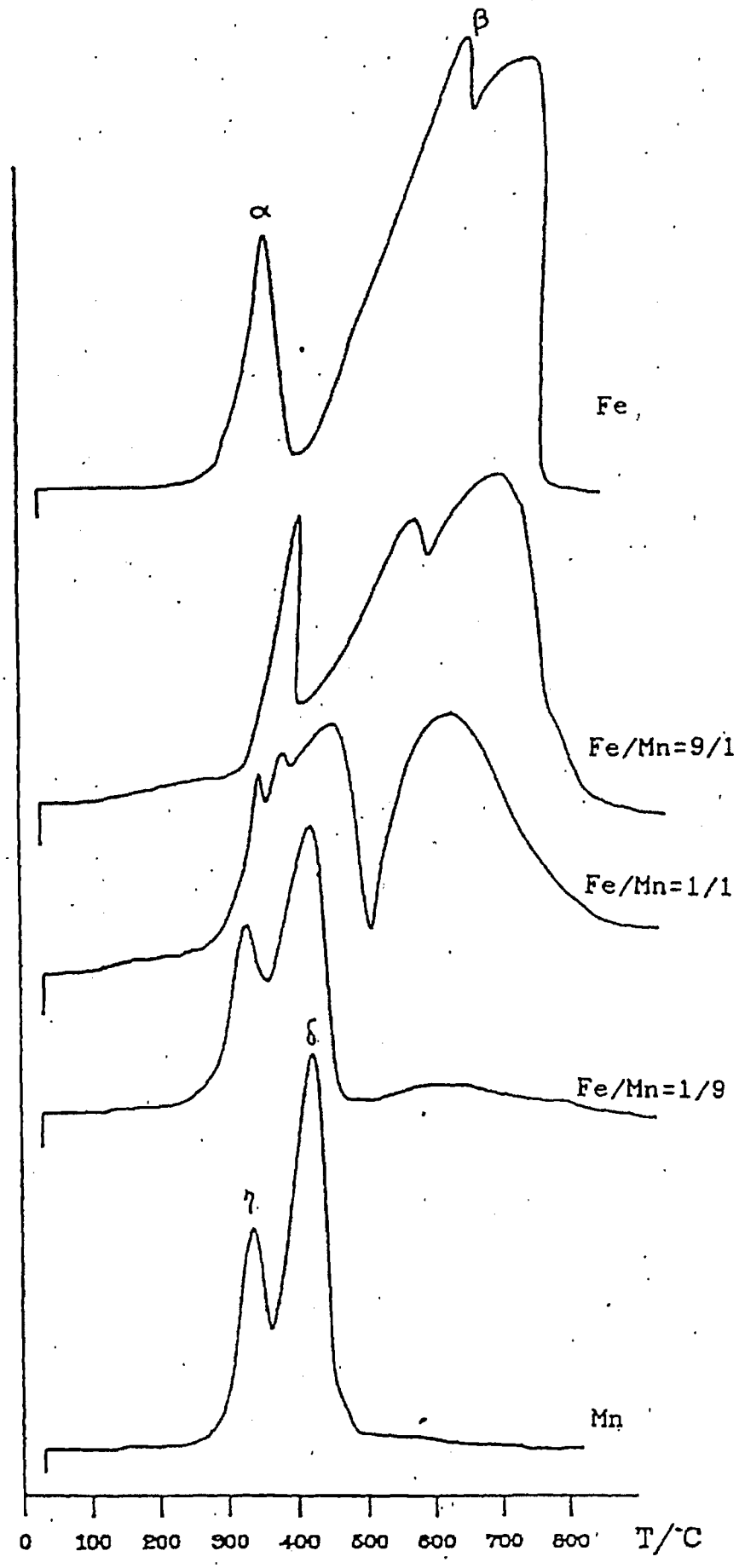

Fig. 18 TPR of catalysts
(calcined at 502 °C in air for 5 hr)

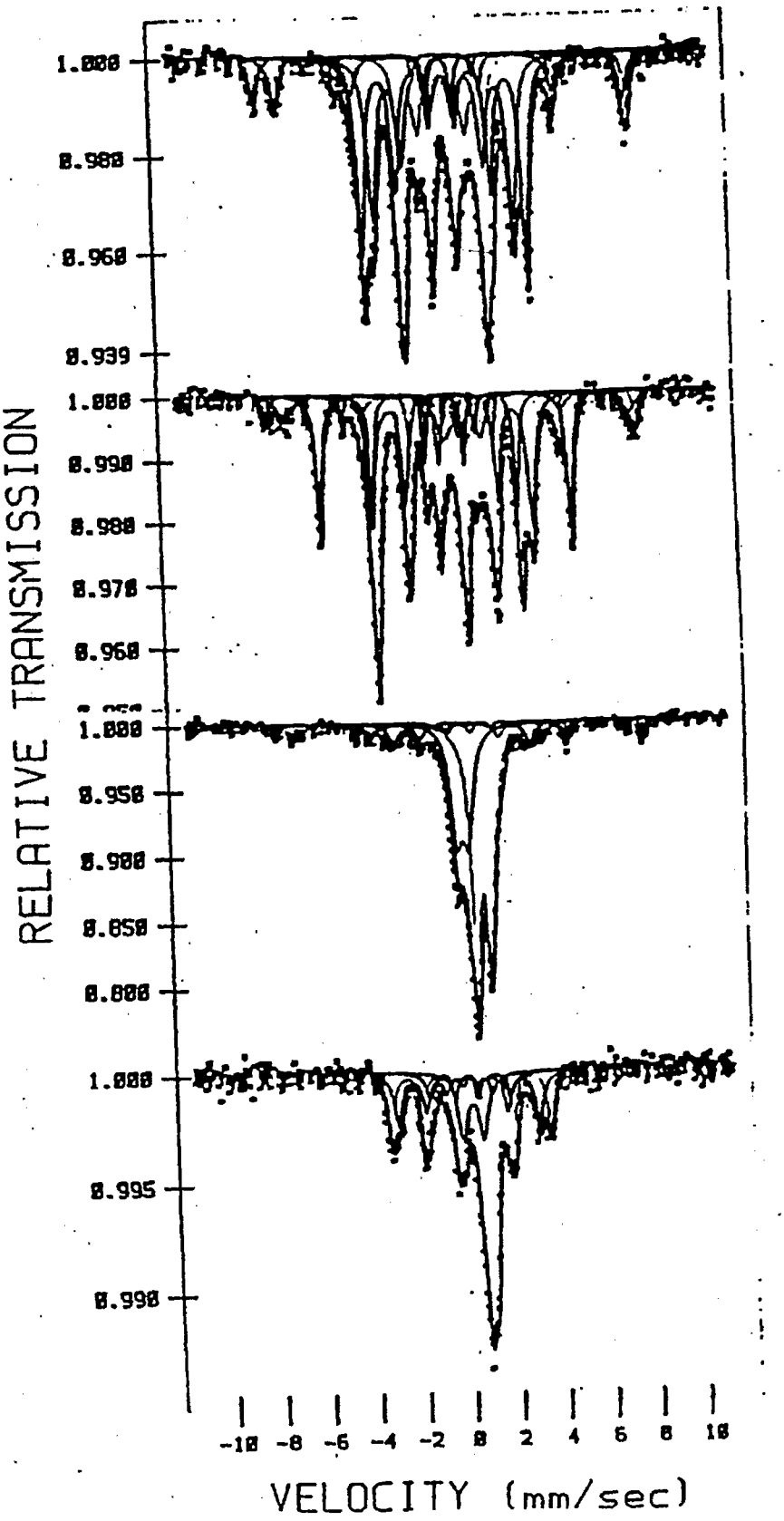

Fig. 19 Mössbauer spectra of 500°C hydrogen reduced Fe-Mn catalysts after CO hydrogenation, from top to bottom, pure iron, Fe/Mn=9/1, Fe/Mn=1/1, Fe/Mn=1/9.

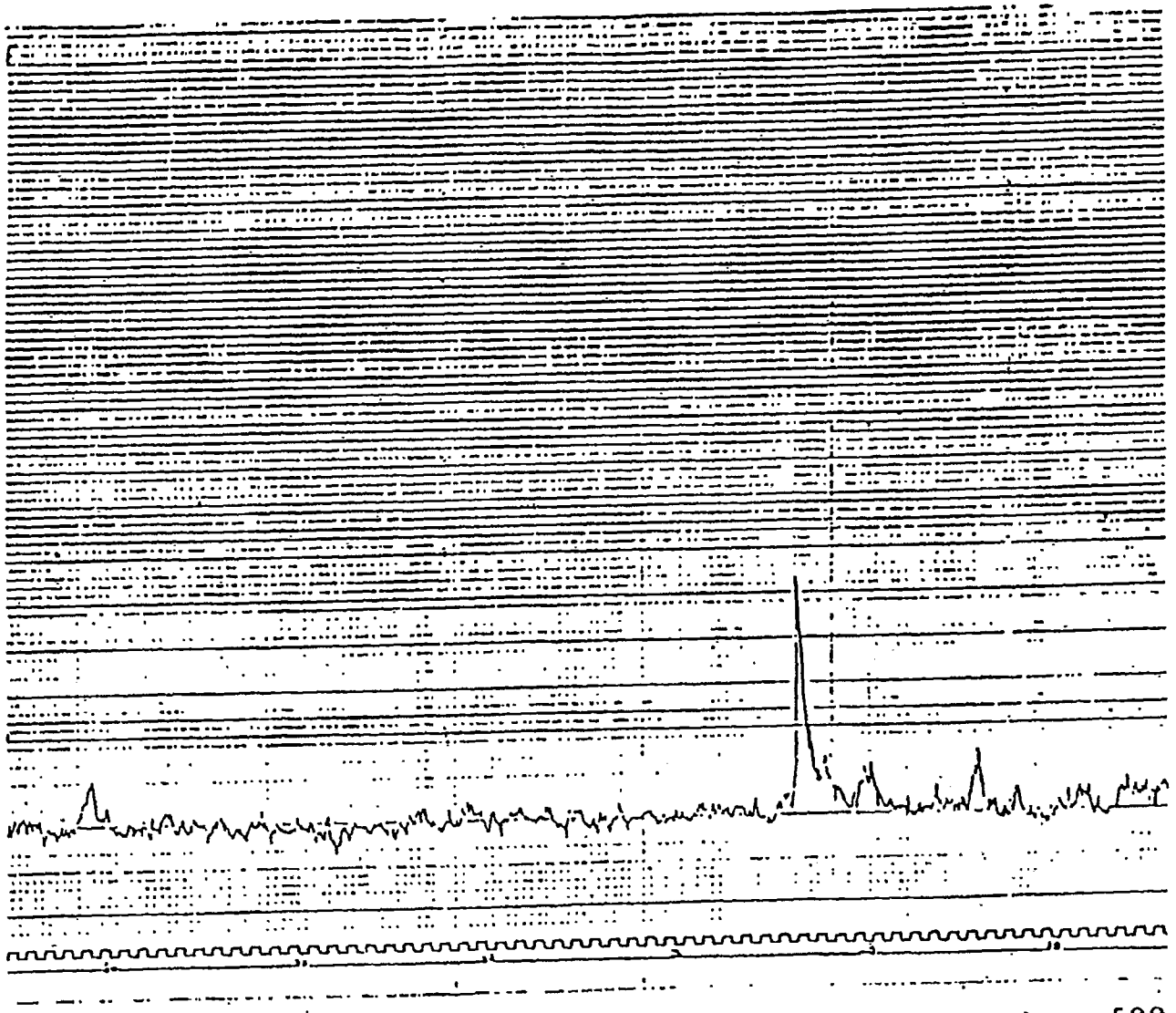

Fig. 20a XRD spectrum of catalyst Fe/Mn=9/1 reduced at 500 C and reacted at 320 C for 20 hrs.

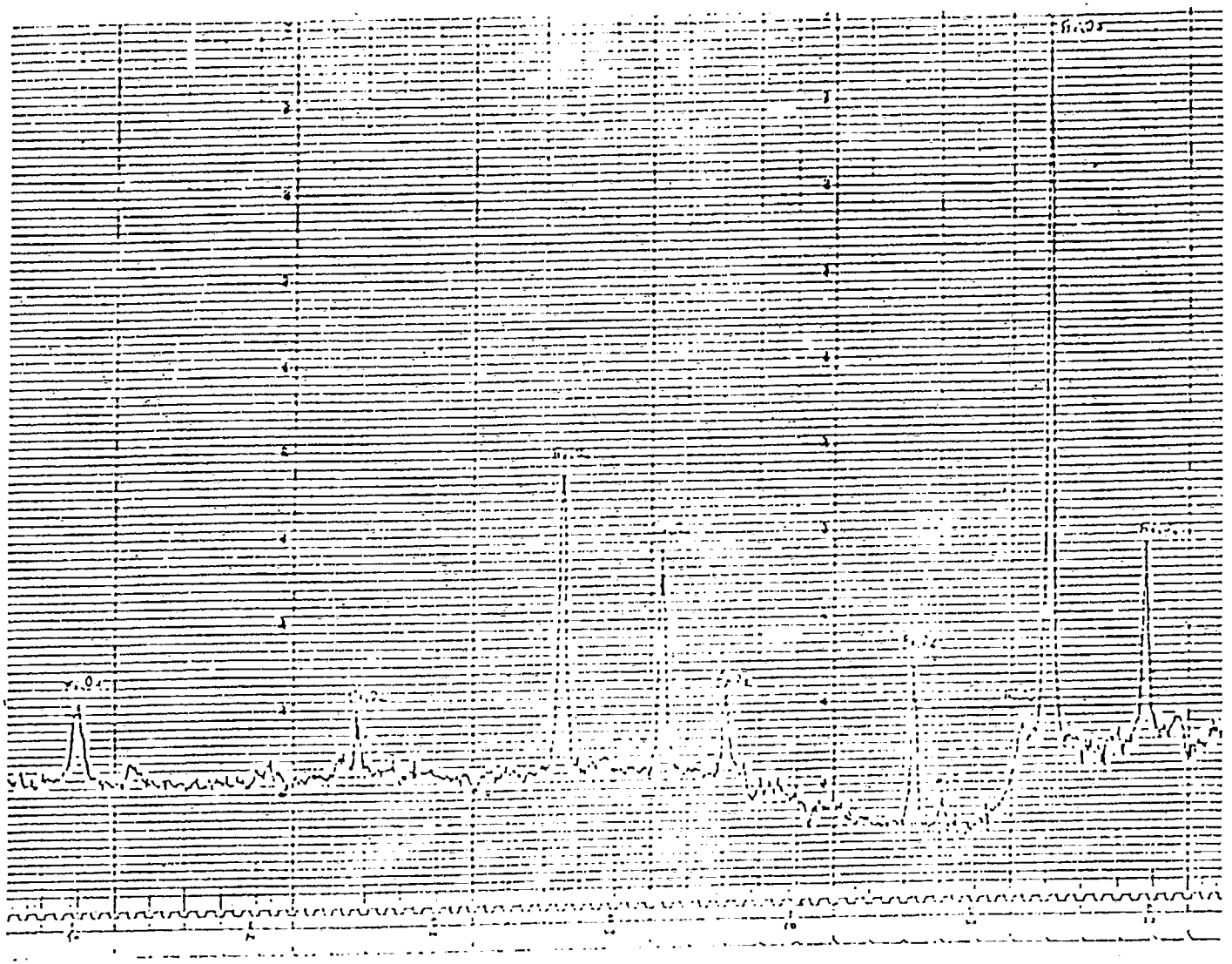

Fig. 20b XRD spectrum of catalyst Fe Mn=9/1 reduced at 350 C and reacted at 320 C for 5 hrs.

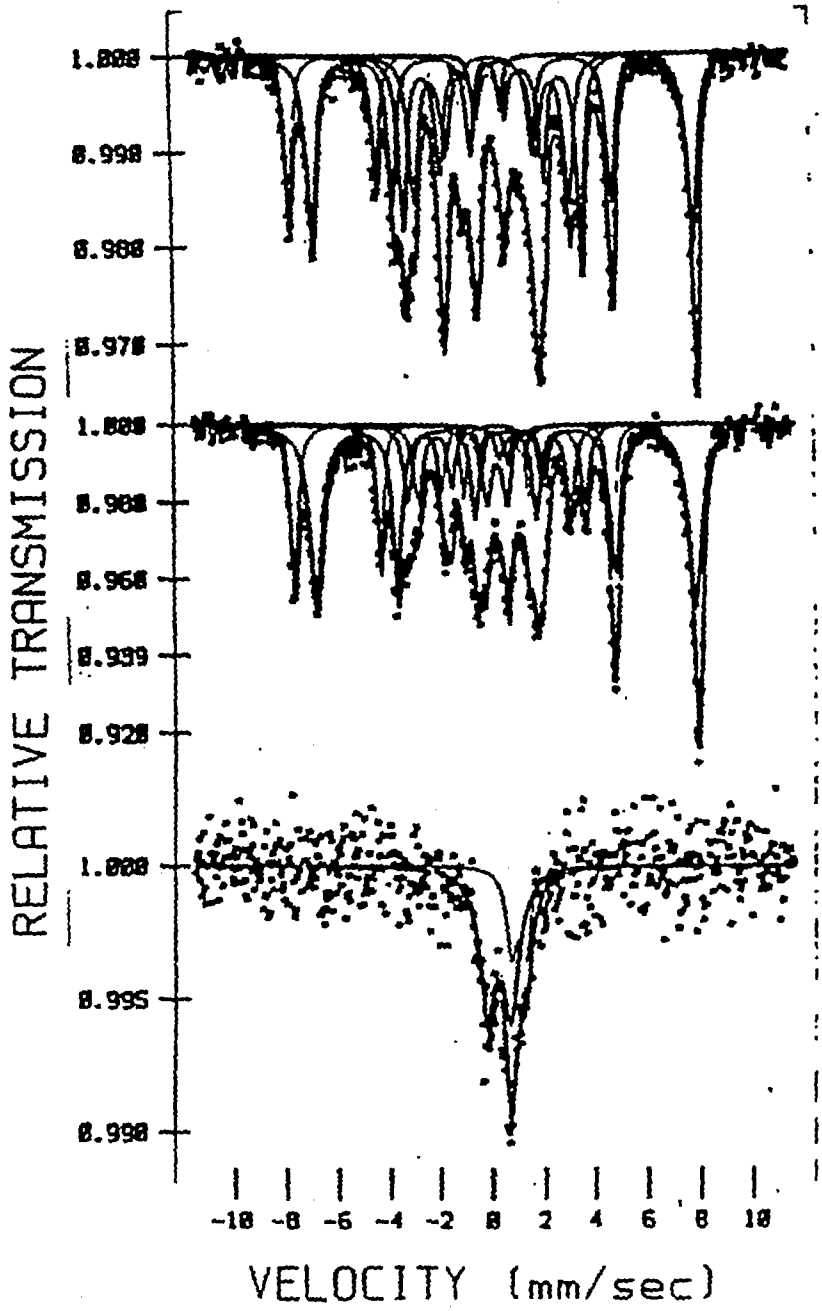

Fig. 21 Mössbauer spectra of 330°C hydrogen reduce
Fe-Mn catalysts after CO hydrogenation, fr
top to bottom, pure iron, Fe/Mn=9/1, Fe/Mn

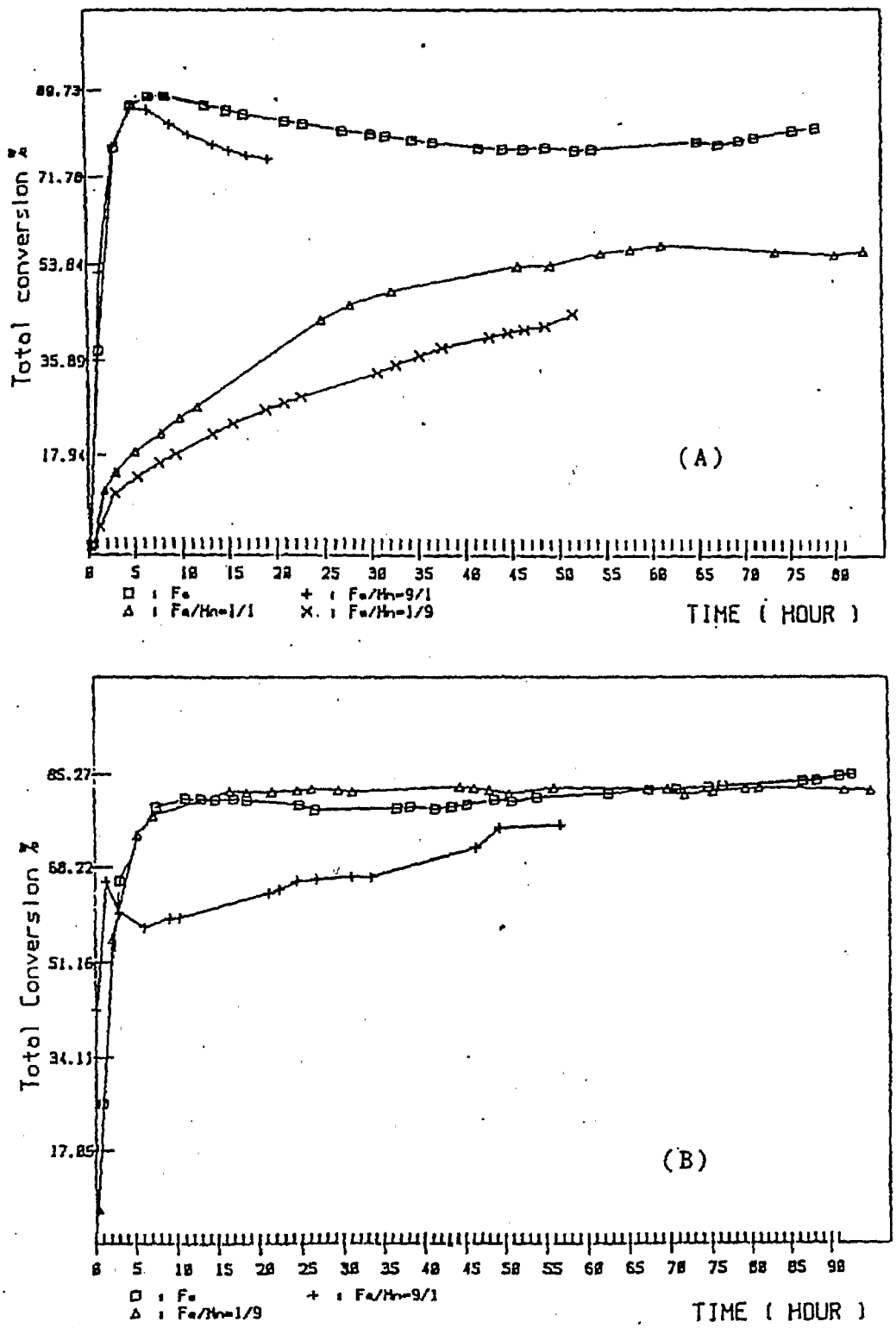

Fig. 22 Variation of conversion with reaction time.
(A) 500 C reduced, (B) 330 C reduced

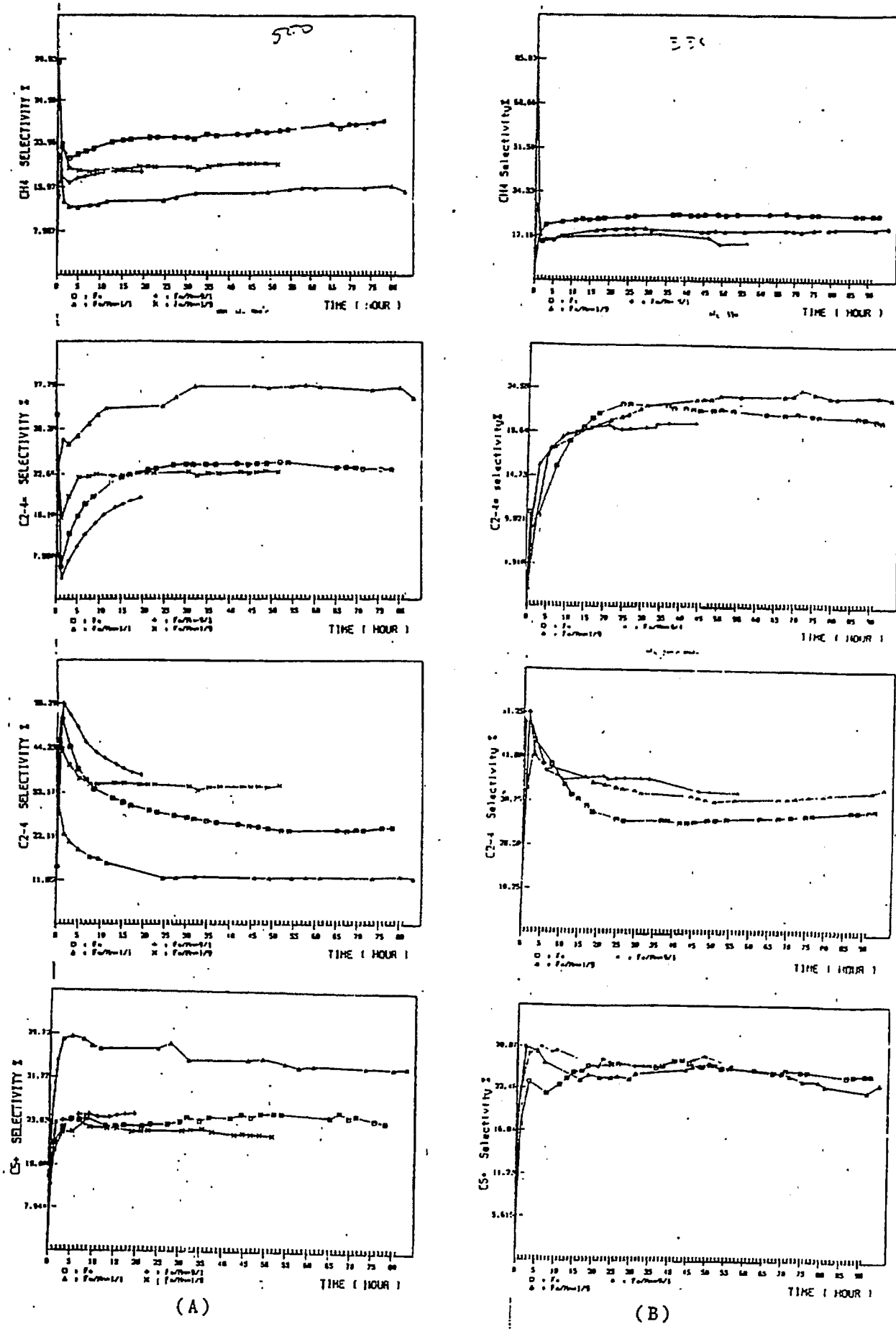

Fig. 23 Variation of selectivity with reaction time.
(A) 500 C reduced, (B) 330 C reduced.

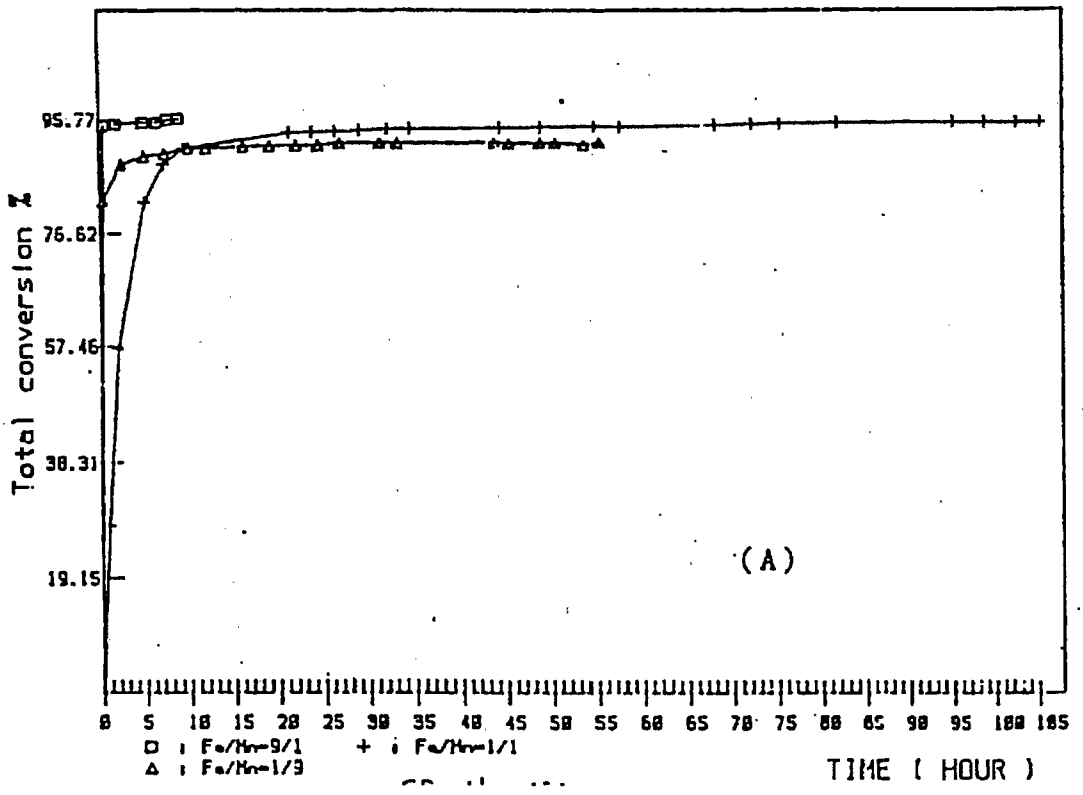

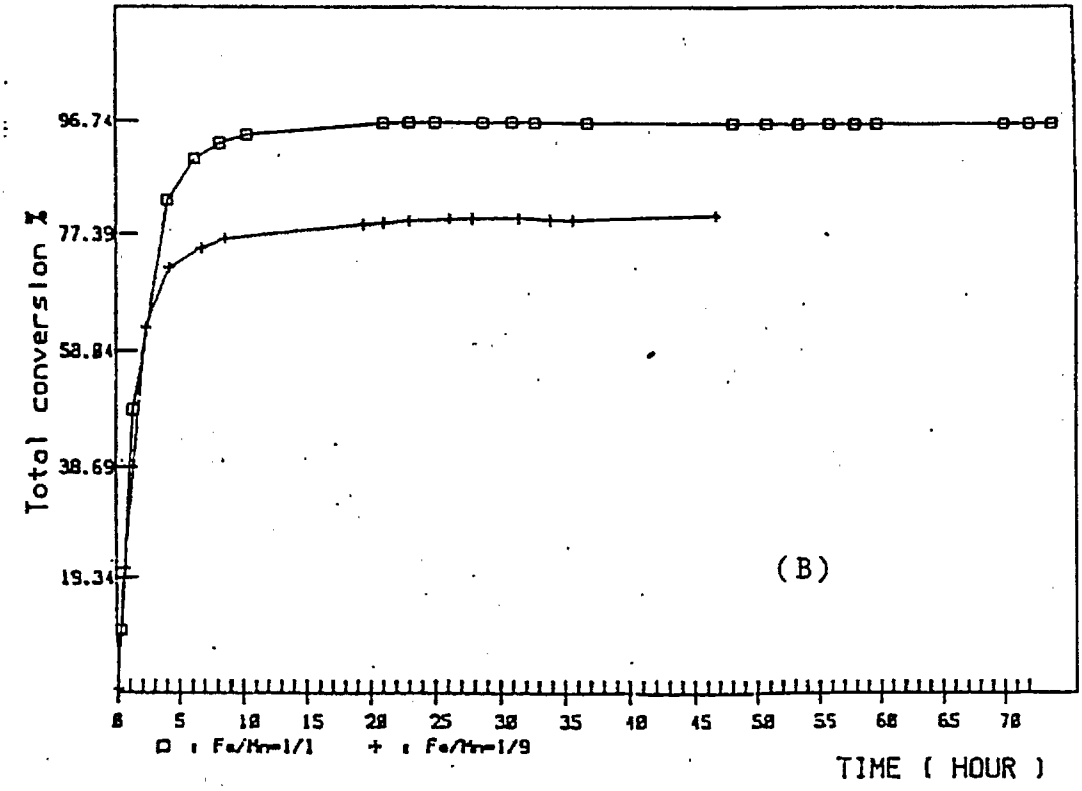

Fig. 24 Variation of conversion with reaction time.
(A) 330 C CO/H2 pretreated,
(B) 270 C CO/H2 pretreated.

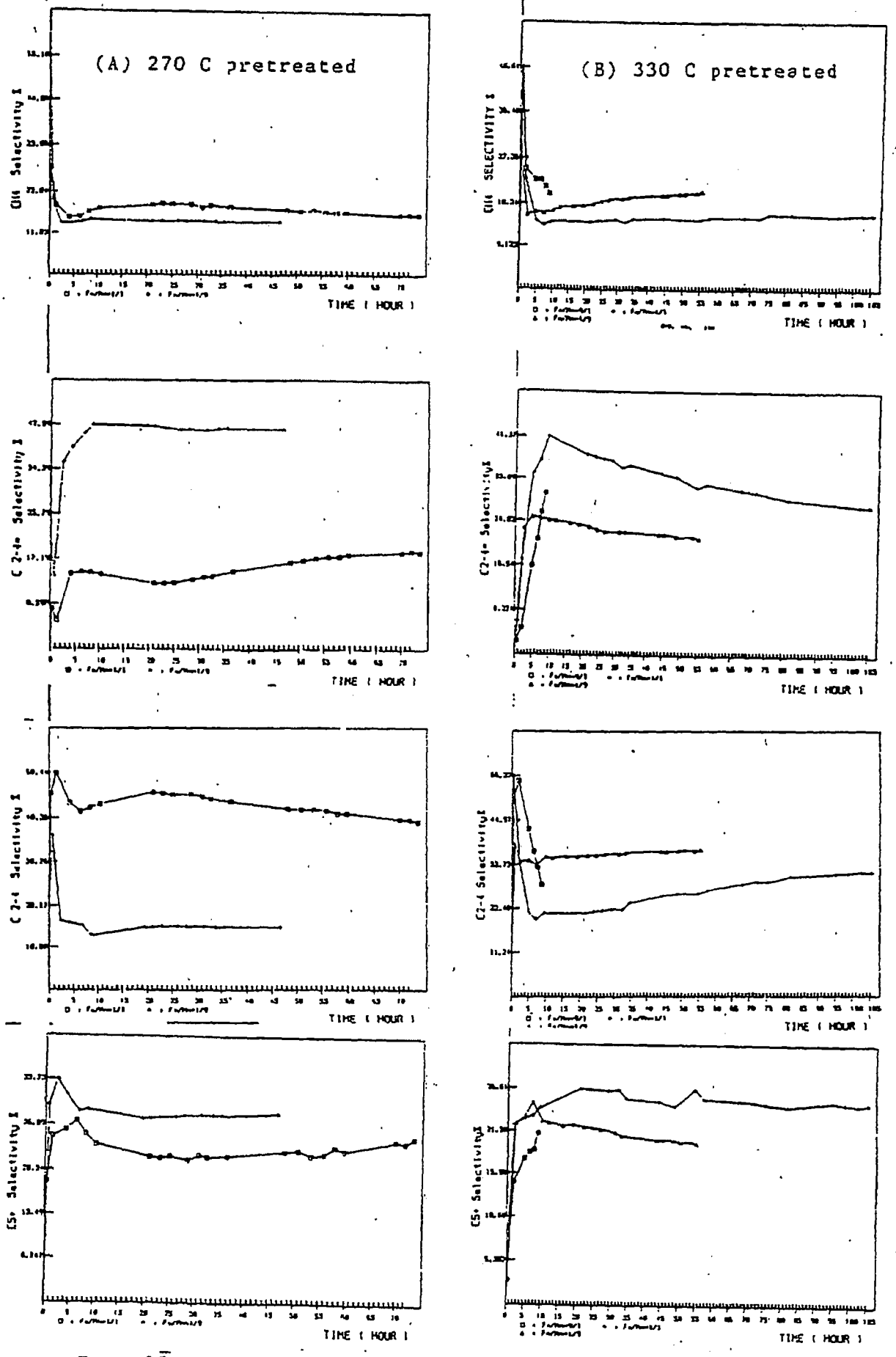

Fig. 25 Variation of selectivity with reaction time.
CO/H2 pretreated catalysts.

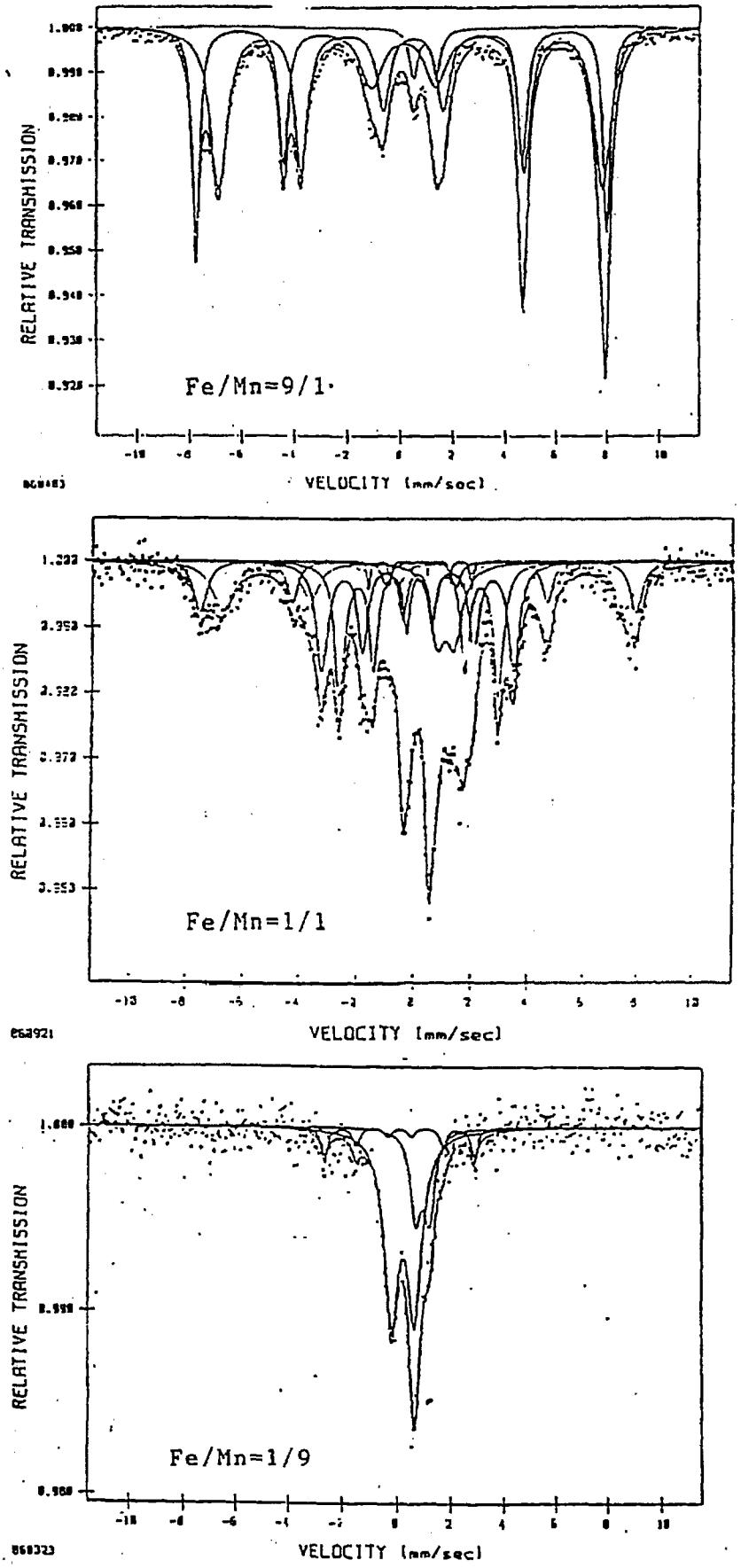

Fig. 26 Mossbauer spectra of 330 C CO/H2 pretreated catalysts after CO hydrogenation.

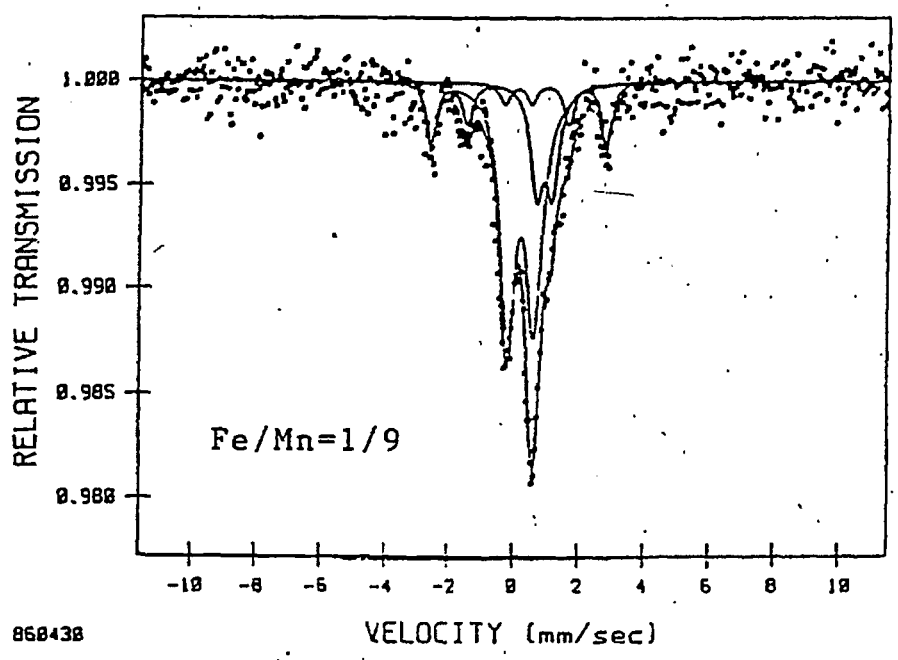

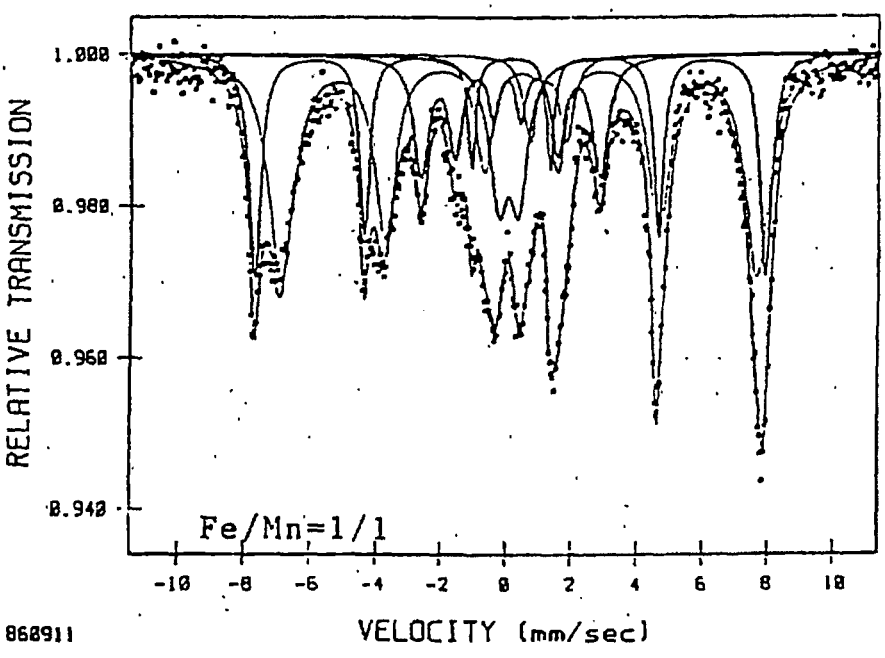

Fig. 27 Mossbauer spectra of 270 C CO/H2 pretreated catalysts after CO hydrogenation.

END

U.S. DEPARTMENT OF COMMERCE
Technology Administration
National Technical Information Service
Springfield, VA 22161 (703) 605-6000